Learning generalized Nash equilibria in monotone games
A hybrid adaptive extremum seeking control approach

Krilašević, Suad; Grammatico, Sergio

DOI
10.1016/j.automatica.2023.110931

Publication date
2023

Document Version
Final published version

Published in
Automatica

Automatica 151 (2023) 110931

Contents lists available at ScienceDirect

Automatica

journal homepage: www.elsevier.com/locate/automatica

Learning generalized Nash equilibria in monotone games: A hybrid adaptive extremum seeking control approach ☆

Suad Krilašević *, Sergio Grammatico

Delft Center for Systems and Control, TU Delft, The Netherlands

ARTICLE INFO

Article history:
Received 24 September 2021
Received in revised form 13 January 2023
Accepted 6 February 2023
Available online xxxx

Keywords:
Generalized Nash equilibrium learning
Multi-agent systems
Extremum seeking control

ABSTRACT

In this paper, we solve the problem of learning a generalized Nash equilibrium (GNE) in merely monotone games. First, we propose a novel continuous semi-decentralized solution algorithm without projections that uses first-order information to compute a GNE with a central coordinator. As the second main contribution, we design a gain adaptation scheme for the previous algorithm in order to alleviate the problem of improper scaling of the cost functions versus the constraints. Third, we propose a data-driven variant of the former algorithm, where each agent estimates their individual pseudogradient via zeroth-order information, namely, measurements of their individual cost function values. Finally, we apply our method to a perturbation amplitude optimization problem in oil extraction engineering.

1. Introduction

Decision problems where self-interested intelligent systems or agents wish to optimize their individual cost objective function arise in many engineering applications, such as charging/ discharging coordination for plug-in electric vehicle (Grammatico, 2017; Ma, Callaway, & Hiskens, 2011), demand-side management in smart grids (Mohsenian-Rad, Wong, Jatskevich, Schober, & Leon-Garcia, 2010; Saad, Han, Poor, & Basar, 2012), robotic formation control (Lin, Qu, & Simaan, 0000), and thermostatically controlled loads (Li, Zhang, Lian, & Kalsi, 2015). The key feature that distinguishes these problems from multi-agent distributed optimization is the fact the cost functions and constraints are coupled together. Currently, one active research area is that of finding (seeking) actions that are self-enforceable, e.g. actions such that no agent has an incentive to unilaterally deviate from - the so-called generalized Nash equilibrium (GNE) (Facchinei & Kanzow, 2010, Eq. 1). Due to the aforementioned coupling, information on other agents must be communicated, observed, or measured in order to compute a GNE algorithmically. The nature of this information can vary from knowing everything (full knowledge of the agent actions) (Yi & Pavel, 2019), estimates based on distributed consensus between the agents (Gadjov & Pavel, 2019), to payoff-based estimates (Frihauf, Krstic, & Basar, 2011; Marden, Arslan, & Shamma, 2009). The latter is of special interest as it requires no dedicated inter-agent communication infrastructure.

Literature review: In payoff-based algorithms, each agent can only measure the value of their cost function but does not necessarily know its analytic form. Many of such algorithms are designed for Nash equilibrium problems (NEPs) with finite action spaces where each agent has a fixed policy that specifies what a player should do under any condition, e.g. Goto, Hatanaka, and Fujita (2012), Marden et al. (2009) and Marden and Shamma (2012). On the other hand, the main component of continuous action space algorithms is the payoff-based (pseudo)gradient estimation scheme. A notable class of payoff-based algorithms called Extremum Seeking Control (ESC) is based on the seminal work by Krstić and Wang (2000). The main idea is to use perturbation signals to "excite" the cost function and estimate its gradient which is then used in a gradient-descent-like algorithm. Since then, various different variants have been proposed (Dürr, Stanković, Ebenbauer and Johansson, 2013; Ghaffari, Krstić, & Nešić, 2012; Grushkovskaya, Zuyev, & Ebenbauer, 2018; Labar, Garone, Kinnaert, & Ebenbauer, 2019; Liao, Manzie, Chapman, & Alpcan, 2019; Liu & Krstić, 2011; Shao, Teel, Tan, Liu, & Wang, 2019). A full-information algorithm where the (pseudo)gradient is known, can be "transformed" into an extremum seeking one if it satisfies some properties, like the continuity of the dynamics, use of only one (pseudo)gradient in the dynamics, appropriate stability of the optimizer/NE, etc. At first, (local) exponential stability of the optimizer/NE was

☆ This work was partially supported by the ERC under research project COSMOS (802348). The material in this paper was partially presented at the 60th IEEE Conference on Decision and Control, December 13-15, 2021, Austin, Texas, USA. This paper was recommended for publication in revised form by Associate Editor Martin Guay under the direction of Editor Miroslav Krstic.

* Corresponding author.
E-mail addresses: s.krilasevic-1@tudelft.nl (S. Krilašević), s.grammatico@tudelft.nl (S. Grammatico).

https://doi.org/10.1016/j.automatica.2023.110931
0005-1098/© 2023 Published by Elsevier Ltd.

assumed or implied with other assumptions Krstić and Wang (2000, Assum. 2.2), Frihauf et al. (2011, Assum. 3.1). Thanks to results in averaging and singular perturbation theory (Sanfelice & Teel, 2011; Wang, Teel, & Nešić, 2012) in the hybrid dynamical systems framework (Goebel, Sanfelice, & Teel, 2012), the assumption was relaxed to just (practical) asymptotic stability (Poveda & Teel, 2017a). Subsequently, extremum seeking algorithms were developed for many different applications, such as event-triggered optimization (Poveda & Teel, 2017b), Nesterov-like accelerated optimization with resetting (Poveda & Li, 2021), optimization of hybrid plants (Poveda et al., 2018), population games (Poveda & Quijano, 2015), N-cluster Nash games (Ye, Hu, & Xu, 2020), fixed-time Nash equilibrium seeking for strongly monotone games (Poveda & Krstić, 2021), Nash equilibrium seeking for merely monotone games (Krilašević & Grammatico, 2021a) and generalized Nash equilibrium seeking in strongly monotone games (Krilašević & Grammatico, 2021b).

GNEPs can be solved efficiently by casting them into a variational inequality (VI) (Facchinei & Pang, 2007, Equ. 1.4.7), and in turn into the problem of finding a zero of an operator (Facchinei & Pang, 2007, Equ. 1.1.3), for which there exists a vast literature (Bauschke, Combettes, et al., 2011). For GNEPs, this operator is the KKT operator, composed of the pseudogradient (whose monotonicity determines the type of the game), dual variables, constraints and their gradients. In the case of merely monotone operators, the most widely used solution algorithms are the forward–backward–forward (Bauschke et al., 2011, Rem. 26.18), the extragradient (Korpelevich, 1976) and the subgradient extragradient (Censor, Gibali, & Reich, 2011). The main drawback of all of these algorithms, with respect to an extremum seeking adaptation, is that they require two pseudogradient computations per iteration. Recently, the golden ratio algorithm has been proven to converge in the monotone case with only one pseudogradient computation (Malitsky, 2019). There also exist continuous-time versions of the aforementioned algorithms, like the forward–backward–forward algorithm (Bot, Csetnek, & Vuong, 2020) and the golden ratio algorithm (Gadjov & Pavel, 2020), albeit without projections in the latter case, rendering it unusable for GNEPs, as projections are essential for the dual dynamics. To the best of our knowledge, in the merely monotone case, there currently exists no continuous-time GNEP algorithm that can be paired with extremum seeking.

Contribution: Motivated by the above literature and open research problem, to the best of our knowledge, we consider and solve the problem of learning (i.e., seeking via zeroth-order information) a GNE in merely monotone games. Specifically, our main technical contributions are summarized next:

- We propose a novel, projection-less continuous-time algorithm for solving GNEPs. Unlike (Gadjov & Pavel, 2020), we consider the presence of shared constraints that are satisfied asymptotically.
- We propose a novel dual variable gain adaptation scheme using the framework of hybrid dynamical systems in order to alleviate the problem of improper scaling of the cost and constraint functions.
- We propose an extremum seeking scheme which exploits the aforementioned properties of the previous algorithms and in turn solves for the first time monotone GNEPs with zeroth-order information feedback.

Comparison with Krilašević and Grammatico (2021a, 2021b): Since here we assume non-strong monotonicity of the pseudogradient mapping, the methodology in Krilašević and Grammatico (2021b) based on the forward–backward splitting is not applicable—see Gadjov and Pavel (2020, Equ. 4) for an example of non-convergence. Furthermore, by incorporating projection-less dual dynamics, here we allow for the presence of constraints, in contrast with the methodology in Krilašević and Grammatico (2021a) which cannot be extended to the constrained case. Thus, in this paper, we develop a novel splitting methodology that solves the issues of non-convergence and coupled feasible set, and consequently addresses a much wider class of equilibrium problems. The hybrid gain adaptation is also novel and not considered in Krilašević and Grammatico (2021a, 2021b).

Notation: The set of real numbers and the set of nonnegative real numbers are denoted by $\mathbb{R}$ and $\mathbb{R}_+$, respectively. Given a set $\mathcal{Z}$, $\mathcal{Z}^n$ denotes the Cartesian product of n sets $\mathcal{Z}$. For a matrix $A \in \mathbb{R}^{n\times m}$, $A^\top$ denotes its transpose. For vectors $x, y \in \mathbb{R}^n$ and $M \in \mathbb{R}^{n\times n}$ a positive semi-definite matrix and $\mathcal{A} \subset \mathbb{R}^n$, $\langle x \mid y\rangle$, $\|x\|$, $\|x\|_M$ and $\|x\|_{\mathcal{A}}$ denote the Euclidean inner product, norm, weighted norm and distance to set respectively. Given N vectors $x_1, \ldots, x_N$, possibly of different dimensions, $\mathrm{col}\,(x_1, \ldots x_N) := \left[x_1^\top, \ldots, x_N^\top\right]^\top$. Collective vectors are denoted in bold, i.e, $\boldsymbol{x} := \mathrm{col}\,(x_1, \ldots, x_N)$ and for each $i = 1, \ldots, N$, $\boldsymbol{x}_{-i} := \mathrm{col}(x_1, \ldots, x_{i-1}, x_{i+1}, \ldots, x_N)$ as they collect vectors from multiple agents. Given N matrices $A_1, A_2, \ldots, A_N$, $\mathrm{blkdiag}\,(A_1, \ldots, A_N)$ denotes the block diagonal matrix with A_i on its diagonal. Given a vector x, $\mathrm{diag}(x)$ represents a diagonal matrix whose diagonal elements are equal to the elements of the vector x. For a function $v : \mathbb{R}^n \times \mathbb{R}^m \to \mathbb{R}$ differentiable in the first argument, we denote the partial gradient vector as $\nabla_x v(x, y) := \mathrm{col}\left(\frac{\partial v(x,y)}{\partial x_1}, \ldots, \frac{\partial v(x,y)}{\partial x_N}\right) \in \mathbb{R}^n$. We use $\mathbb{S}^1 := \left\{z \in \mathbb{R}^2 : z_1^2 + z_2^2 = 1\right\}$ to denote the unit circle in $\mathbb{R}^2$. The set-valued mapping $\mathrm{N}_S : \mathbb{R}^n \rightrightarrows \mathbb{R}^n$ denotes the normal cone operator for the set $S \subseteq \mathbb{R}^n$, i.e., $\mathrm{N}_S(x) = \varnothing$ if $x \notin S$, $\left\{v \in \mathbb{R}^n \mid \sup_{z\in S} v^\top(z - x) \le 0\right\}$ otherwise. Id is the identity operator; I_n is the identity matrix of dimension n and $\mathbf{0}_n$ is vector column of n zeros; their index is omitted where the dimensions can be deduced from context. The unit ball of appropriate dimensions depending on context is denoted with $\mathbb{B}$. A continuous function $\gamma : \mathbb{R}_+ \to \mathbb{R}_+$ is of class $\mathcal{K}$ if it is zero at zero and strictly increasing. A continuous function $\alpha : \mathbb{R}_+ \to \mathbb{R}_+$ is of class $\mathcal{L}$ if is non-increasing and converges to zero as its arguments grows unbounded. A continuous function $\beta : \mathbb{R}_+ \times \mathbb{R}_+ \to \mathbb{R}_+$ is of class $\mathcal{KL}$ if it is of class $\mathcal{K}$ in the first argument and of class $\mathcal{L}$ in the second argument. A function $\omega : \mathcal{B}_{\mathcal{A}} \to \mathbb{R}_+$ is a proper indicator of $\mathcal{A}$ on $\mathcal{B}_{\mathcal{A}}$ if it is continuous, if $\omega(x_i)$ approaches infinity when i approaches infinity if either $\|x_i\|$ approaches infinity or x_i approaches the boundary of set $\mathcal{A}$, and $\omega(x) = 0$ if and only if $x \in \mathcal{A}$ (Poveda et al., 2018).

The framework of hybrid dynamical systems (HDS) theory (Goebel et al., 2012) like Sanfelice and Teel (2011), Poveda and Teel (2017a, Lemma 4) and Wang et al. (2012) is especially attractive for extremum seeking, as it allows one to quickly and elegantly prove various stability theorems (Poveda & Krstić, 2021; Poveda & Li, 2021; Poveda & Teel, 2017a, 2017b). Thus, we also use the framework of HDSs to model our algorithms. An HDS is defined as

$$\dot{x} \in F(x) \qquad \text{if} \quad x \in C \tag{1a}$$

$$x^+ \in G(x) \qquad \text{if} \quad x \in D, \tag{1b}$$

where $x \in \mathbb{R}^n$ is the state, $F : \mathbb{R}^n \to \mathbb{R}^n$ is the flow map, and $G : \mathbb{R}^n \to \mathbb{R}^n$ is the jump map, the sets C and D, are the flow set and the jump set, respectively, that characterize the points in space where the system evolves according to (1a), or (1b), respectively. The data of the HDS is defined as $\mathcal{H} := \{C, D, F, G\}$. Solutions $x : \mathrm{dom}(x) \to \mathbb{R}^n$ to (1) are defined on hybrid time domains, and they are parameterized by a continuous-time index $t \in \mathbb{R}_+$ and a discrete-time index $j \in \mathbb{Z}_+$. Solutions with unbounded time or index domains are said to be complete (Goebel et al., 2012, Chp. 2). We now define the sufficient hybrid basic conditions that enable the use of various results from HDS theory (Goebel et al., 2012, Assum. 6.5).

Definition 1 (*Hybrid Basic Conditions*)**.** A HDS in (1) is said to satisfy the Hybrid basic conditions if C and D are closed, $C \subset \text{dom}(F)$, $D \subset \text{dom}(G)$, F and G are continuous on C and D respectively. □

2. Generalized Nash equilibrium problem

We consider a multi-agent system with N agents indexed by $i \in \mathcal{I} := \{1, 2, \dots N\}$, each with cost function

$$J_i(u_i, \boldsymbol{u}_{-i}), \tag{2}$$

where $u_i \in \mathbb{R}^{m_i}$ is the decision variable, $J_i : \mathbb{R}^{m_i} \times \mathbb{R}^{m_{-i}} \to \mathbb{R}$. Let us also define $m := \sum_{j \in \mathcal{I}} m_j$ and $m_{-i} := \sum_{j \neq i} m_j$. Formally, we do not consider local constraints as in Krilašević and Grammatico (2021a), Poveda and Krstić (2021) and Ye et al. (2020), but they could be approximated softly via penalty-barrier functions into the cost function. All agents are subject to convex coupling constraints $g_j(\boldsymbol{u})$ indexed by $j \in \mathcal{Q} := \{1, 2, \dots q\}$. Therefore, let us denote the overall feasible decision set as

$$\boldsymbol{\mathcal{U}} := \left\{ \boldsymbol{u} \in \mathbb{R}^m \mid g(\boldsymbol{u}) \le \boldsymbol{0} \right\}, \tag{3}$$

and the feasible set of agent i as

$$\mathcal{U}_i(\boldsymbol{u}_{-i}) := \left\{ u_i \in \mathbb{R}^{m_i} \mid g(\boldsymbol{u}) \le \boldsymbol{0} \right\}, \tag{4}$$

where $g(\boldsymbol{u}) = \text{col}\left((g_j(\boldsymbol{u}))_{j \in \mathcal{Q}} \right)$.

The goal of each agent is to minimize its cost function, i.e.,

$$\forall i \in \mathcal{I} : \min_{u_i \in \mathcal{U}_i(\boldsymbol{u}_{-i})} J_i(u_i, \boldsymbol{u}_{-i}), \tag{5}$$

which depends on the decision variables of other agents as well. Thus, a game $\mathcal{G}$ is defined by the set of cost functions and the feasible set, i.e. $\mathcal{G} := \{(J_i(\boldsymbol{u}))_{i \in \mathcal{I}}, (g_j(\boldsymbol{u}))_{j \in \mathcal{Q}}\}$. From a game-theoretic perspective, this is the problem to compute a generalized Nash equilibrium (GNE), as formalized next.

Definition 2 (*Generalized Nash Equilibrium*)**.** A set of control actions $\boldsymbol{u}^* := \text{col}\left(u_i^*\right)_{i \in \mathcal{I}}$ is a generalized Nash equilibrium if, for all $i \in \mathcal{I}$,

$$u_i^* \in \underset{v_i}{\text{argmin}}\, J_i\left(v_i, \boldsymbol{u}_{-i}^*\right) \text{ s.t. } \left(v_i, \boldsymbol{u}_{-i}^*\right) \in \boldsymbol{\mathcal{U}}. \tag{6}$$

with J_i as in (2) and $\boldsymbol{\mathcal{U}}$ as in (3). □

In plain words, a set of inputs is a GNE if no agent can improve its cost function by unilaterally changing its input.

A common approach for solving a GNEP is to translate it into a quasi-variational inequality (QVI) (Facchinei & Kanzow, 2010, Thm. 3.3) that can be simplified to a variational inequality (VI) (Facchinei & Kanzow, 2010, Thm. 3.9) for a certain subset of solutions called variational-GNE (v-GNE), which in turn can be translated into a problem of finding zeros of a monotone operator (Facchinei & Pang, 2007, Equ. 1.1.3). To ensure the equivalence of the GNEP and QVI, we postulate the following assumption (Facchinei & Kanzow, 2010, Thm. 3.3):

Standing Assumption 1 (*Regularity*)**.** For each $i \in \mathcal{I}$, the function J_i in (2) is differentiable and its gradient is locally Lipschitz continuous; the function $J_i(\cdot, \boldsymbol{u}_{-i})$ is convex for every $\boldsymbol{u}_{-i}$; For each $j \in \mathcal{Q}$, convex constraint $g_j(\boldsymbol{u})$ is continuously differentiable, $\boldsymbol{\mathcal{U}}$ is non-empty and satisfies Slater's constraint qualification. □

We focus on a subclass of GNE called variational GNE (Facchinei & Kanzow, 2010, Def. 3.10). A collective decision $\boldsymbol{u}^*$ is a v-GNE in (6) if and only if there exists a dual variable $\lambda^* \in \mathbb{R}^q$ such that the following KKT conditions are satisfied (Facchinei & Kanzow, 2010, Th. 4.8):

$$\boldsymbol{0}_{m+q} \in F_{\text{ex}}(\boldsymbol{u}^*, \lambda^*) := \begin{bmatrix} F(\boldsymbol{u}^*) + \nabla g(\boldsymbol{u}^*)^\top \lambda^* \\ -g(\boldsymbol{u}^*) + \text{N}_{\mathbb{R}^q_+}(\lambda^*) \end{bmatrix}, \tag{7}$$

where by stacking the partial gradients $\nabla_{u_i} J_i(u_i, \boldsymbol{u}_{-i})$ into a single vector, we have the so-called pseudogradient mapping:

$$F(\boldsymbol{u}) := \text{col}\left(\left(\nabla_{u_i} J_i\left(u_i, \boldsymbol{u}_{-i}\right) \right)_{i \in \mathcal{I}} \right). \tag{8}$$

Let us also postulate the weakest working assumption in GNEPs with continuous actions, i.e. the monotonicity of the pseudogradient mapping (Facchinei & Pang, 2007, Def. 2.3.1, Thm. 2.3.4):

Standing Assumption 2 (*Monotonicity*)**.** The pseudogradient mapping F in (8) is monotone, i.e., it holds that

$$\inf_{\boldsymbol{u}, \boldsymbol{v} \in \text{dom} F} \langle \boldsymbol{u} - \boldsymbol{v} \mid F(\boldsymbol{u}) - F(\boldsymbol{v}) \rangle \ge 0. \quad \square$$

The regularity and monotonicity assumptions are not enough to ensure the existence of a v-GNE Facchinei and Pang (2007, Thm. 2.3.3, Corr. 2.2.5), Facchinei and Kanzow (2010, Thm. 6), hence let us postulate its existence:

Standing Assumption 3 (*Existence*)**.** There exists $\omega^* := \text{col}(\boldsymbol{u}^*, \lambda^*) \in \mathbb{R}^m \times \mathbb{R}^q_+$ such that Eq. (7) is satisfied. □

In this paper, we consider the problem of finding a v-GNE of the game in (5) via zeroth-order information, i.e. local measurements of the cost functions in (2).

3. Full-information generalized Nash equilibrium seeking

We present two novel full-information GNE seeking algorithms. In the first algorithm, the dual variables are calculated without the use of projections by a central coordinator. The lack of projections onto tangent cones, along with the fact that the flow map of the algorithm contains only one pseudogradient computation and that the algorithm itself converges merely under the monotonicity assumption, enables us to use hybrid dynamical system theory for the zeroth-order extension of the algorithm later on. In the second algorithm, we propose a hybrid gain adaptation scheme, in order to improve the performance of the algorithm when we do not know a priori how to best tune the gains.

3.1. Projection-less GNE seeking algorithm

The algorithm in Gadjov and Pavel (2020) proves convergence to a NE for a monotone pseudogradient by combining additional filtering dynamics and state z with the standard NE seeking one. Similarly, we propose a Lagrangian first-order primal dynamics with filtering for each agent:

$$\begin{bmatrix} \dot{u}_i \\ \dot{z}_i \end{bmatrix} = \begin{bmatrix} -u_i + z_i - \gamma_i\left(\nabla_{u_i} J_i(u_i, \boldsymbol{u}_{-i}) + \nabla_{u_i} g(\boldsymbol{u})^\top \lambda \right) \\ -z_i + u_i \end{bmatrix}.$$

The authors in Gadjov and Pavel (2020) propose a passivity framework for the convergence of their golden-ratio inspired algorithm. Instead, we offer a different intuition for convergence. Via the invariance theorem, it follows that the stable equilibrium points must be in the Lyapunov invariant set. Without the additional dynamics and under the monotonicity assumption, the invariant set would cover the whole flow set. With the filtering dynamics, the invariant set is restricted to the points where the flow map is equal to zero. In the case of the dual dynamics, in order to avoid projections, we propose the following dynamics:

$$\begin{aligned} \forall j \in \mathcal{Q} : \dot{\lambda}_j &= \lambda_j \left(g_j(\boldsymbol{u}) - \lambda_j + w_j \right) \\ \dot{w} &= -w + \lambda. \end{aligned} \tag{9}$$

While the classic dual Lagrangian dynamics preserve the positivity of the dual variables by projecting onto the positive orthant,

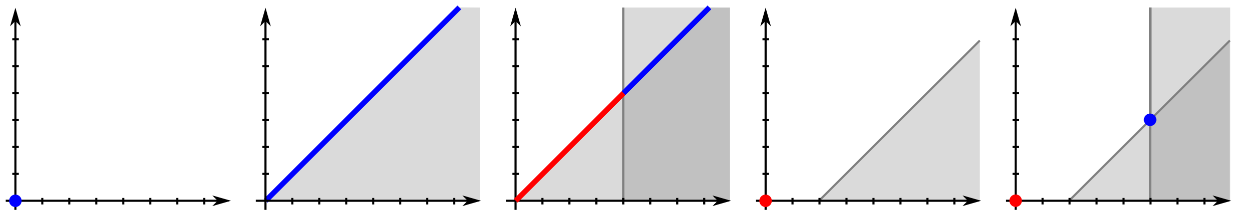

(a) $\mathcal{A}$ (blue dot) contains a single point.

(b) $\mathcal{A}$ (blue line) contains multiple points.

(c) $\mathcal{A}$ (blue line) and $\mathcal{M} \setminus \mathcal{A}$ (red line) are connected.

(d) $\mathcal{A}$ contains no points, set $\mathcal{M}$ (red dot) is a single point.

(e) $\mathcal{A}$ (blue dot) and $\mathcal{M} \setminus \mathcal{A}$ (red dot) disconnected.

Fig. 1. The figures represent projections of the sets $\mathcal{M}$ and $\mathcal{A}$ onto the subspace of $\boldsymbol{u}$ coordinates with $F(\boldsymbol{u}) := \mathrm{col}\,(u_2, -u_1)$: $\mathcal{A}$ is shown in blue, while the other equilibrium points of (10) $\mathcal{M} \setminus \mathcal{A}$, are shown in red. Areas that satisfy the constraints are shown in gray. The set $\mathcal{M}$ is not necessarily connected as shown in Fig. 1(e). Without constraints, $\mathcal{M}$ is equivalent to $\mathcal{A}$ and it contains only the zeros of the pseudogradient as shown in Fig. 1(a). By adding constraints, we can either create new equilibrium solutions (Figs. 1(b), 1(e)) or "remove" previous ones (Fig. 1(d)). Either way, "all" the solutions are still included in the set $\mathcal{M}$, which is the union of all solutions to games $\{(J_i(\boldsymbol{u}))_{i\in\mathcal{I}}, (g_j(\boldsymbol{u}))_{j\in\tilde{\mathcal{Q}}}\}$, where $\tilde{\mathcal{Q}}$ is a subset of $\mathcal{Q}$. (For interpretation of the references to color in this figure legend, the reader is referred to the web version of this article.)

the same is accomplished in (9) by multiplying the "standard" dual dynamics of each individual variable with the dual variable. Consequentially, a positive dual variable cannot become negative over time as it cannot cross zero. Unlike (Dürr & Ebenbauer, 2011; Dürr, Zeng and Ebenbauer, 2013), where strict convexity of the cost and constraint functions is assumed to avoid having the invariant set be equivalent to the entire flow set, thanks to our newfound understanding of the filtering dynamics, we can incorporate them to relax the strict convexity assumption.

Thus, in collective form, we have

$$\dot{\omega} = \begin{bmatrix} \dot{\boldsymbol{u}} \\ \dot{\boldsymbol{z}} \\ \dot{\lambda} \\ \dot{w} \end{bmatrix} = \begin{bmatrix} -\boldsymbol{u} + \boldsymbol{z} - \Gamma(F(\boldsymbol{u}) + \nabla g(\boldsymbol{u})^\top \lambda) \\ -\boldsymbol{z} + \boldsymbol{u} \\ \mathrm{diag}\,(\lambda)\,(g(\boldsymbol{u}) - \lambda + w) \\ -w + \lambda \end{bmatrix}. \tag{10}$$

To properly understand the behavior of this system, we first need to define the key sets. Let us define the set of equilibrium points of the dynamics in (10) as

$$\mathcal{M} := \Big\{\omega \in \mathbb{R}^{2m} \times \mathbb{R}^{2q}_{+} \mid \boldsymbol{u} = \boldsymbol{z},\, w = \lambda,\, \boldsymbol{0}_m = F\,(\boldsymbol{u}) + \nabla g(\boldsymbol{u})^\top \lambda,\, \mathrm{diag}\,(\lambda)\,\mathrm{diag}\,(g(\boldsymbol{u})) = 0\Big\}, \tag{11}$$

its subset $\mathcal{A}$ which relates to the solutions of the game in (5) as

$$\mathcal{A} := \Big\{\omega \in \mathbb{R}^{2m} \times \mathbb{R}^{2q}_{+} \mid \boldsymbol{u} = \boldsymbol{z},\, w = \lambda,\, \boldsymbol{0}_m \in F_{\mathrm{ex}}\,(\boldsymbol{u}, \lambda)\Big\} \subseteq \mathcal{M}, \tag{12}$$

and $\mathcal{L}$ as the set where at least one dual variable is equal to zero:

$$\mathcal{L} := \{\omega \in \mathbb{R}^{2m} \times \mathbb{R}^{2q}_{+} \mid \lambda_1 \cdot \lambda_2 \cdot \ldots \cdot \lambda_q = 0\}.$$

Let us make a few key observations. Firstly, not all equilibrium points in $\mathcal{M}$ are related to the solutions of the GNEP like the points in $\mathcal{A}$ (see Figs. 1(c), 1(d), 1(e)). Secondly, if the dynamics are initiated in the set $\mathcal{L}$, then the dual variables initiated with zero will stay zero for the whole trajectory. Thus, such trajectories do not converge to the solution unless the dual variables are initialized correctly. To avoid this problem, it is sufficient to initialize the trajectories outside of $\mathcal{L}$. To further understand the properties of these sets, we show some examples in Fig. 1. We later show that $\mathcal{M}$ is attractive. Additionally, the following Lemma characterizes the stability of points in $\mathcal{M} \setminus \mathcal{A}$.

Lemma 1. *Let the Standing Assumptions hold. Then, the equilibrium points in $\mathcal{M} \setminus \mathcal{A}$ are unstable for dynamics in (10).*

Proof. See Appendix B. ■

Therefore, in order to prove the stability of $\mathcal{A}$, we need the sets $\mathcal{A}$ and $\mathcal{M} \setminus \mathcal{A}$ to be disjoint, as the latter is the set of undesired equilibria. In Figs. 1(b) and 1(c) we illustrate this situation happens when the solution set contains multiple points and some of them are "removed" by the introduction of the new constraints. Thus, we have to assume this is not the case:

Standing Assumption 4 (*Isolation of Solutions*). By removing constraints that are not active in the solution set $\mathcal{A}$ (for which $\lambda_j^* = 0$) from the overall feasible decision set $\boldsymbol{\mathcal{U}}$ in (3), additional solutions that are connected to $\mathcal{A}$ are not created. □

We note that this assumption fails only in very specific conditions. For example, let $F(\boldsymbol{u}) = \mathrm{col}\,(u_2, -u_1)$, $g_1(\boldsymbol{u}) = a_1 u_1 + b_1 u_2 + c_1$ and $g_2(\boldsymbol{u}) = a_2 u_1 + b_2 u_2 + c_2$. Standard Assumption 4 fails only if $c_1 = 0$ or $c_2 = 0$. Even if Standard Assumption 4 is not satisfied, by Lemma 1 the equilibrium points in $\mathcal{M} \setminus \mathcal{A}$ are unstable, hence there would be no problem in practice.

Since we cannot claim attractivity from all points in the domain, we should use the notion of local stability, as formalized next.

Definition 3 (*UL(p)AS and UG(p)AS* Poveda et al., 2018**).** A compact set $\mathcal{A} \subset \mathbb{R}^n$ is said to be Uniformly Locally pre-Asymptotically Stable (ULpAS) with basin of attraction $\mathcal{B}_\mathcal{A}$ if for every proper indicator $\omega(\cdot)$ of $\mathcal{A}$ on $\mathcal{B}_\mathcal{A}$ there exists $\beta \in \mathcal{KL}$ such that any solution x of $\mathcal{H}$ with $x(0,0) \in \mathcal{B}_\mathcal{A}$ satisfies $\omega(x(t,j)) \le \beta(\omega(x(0,0)), t+j)$, for all $(t,j) \in \mathrm{dom}(x)$. If this bound holds with $\omega(\cdot)$ replaced by $\|\cdot\|_\mathcal{A}$, and for all $x(0,0) \in C \cup D$, the set $\mathcal{A}$ is said to be Uniformly Globally pre-Asymptotically Stable (UGpAS). If additionally all solutions are complete, we then use the acronyms ULAS and UGAS respectively.

Finally, we show that the dynamics in (10) converge to the solutions of the game in (5), if the initial value of the dual variables is different from zero, as formalized next:

Theorem 1. *Let the Standing Assumptions hold and consider the system dynamics in (10). The set $\mathcal{A}$ in (12) is ULAS with basin of attraction $(\mathbb{R}^{2m} \times \mathbb{R}^{2q}_{+} \setminus \mathcal{L}) \cup \mathcal{A}$.* □

Proof. See Appendix A. ■

Remark 1. It is mathematically also possible to derive a distributed (center-free) implementation of our semi-decentralized algorithm, similarly to Krilašević and Grammatico (2021b, Equ. 14), where each agent estimates the dual variables using the information exchanged with the neighbors. While technically possible, this approach is less in line with the almost-decentralized philosophy of extremum seeking, since it would require a dedicated communication network.

3.2. Hybrid adaptive gain

It is known that primal–dual dynamics satisfy the constraints only asymptotically, thus they allow for constraint violation in the transient (Bianchi & Grammatico, 2021; Yi & Pavel, 2019). Such behavior might happen for longer periods of time if the norm of the pseudogradient $F(\boldsymbol{u})$ is "dominant" over that of the gradient of the constraint vector, $\nabla g(\boldsymbol{u})$. Furthermore, as the zeroth-order variant from Section 4 introduces perturbations to the primal dynamics, it can happen that the perturbations "overpower" either the pseudogradient or the constraint part of the dynamics, thus hindering the convergence to the solution for a wide set of perturbation amplitude parameters. Therefore, to reduce the violation behavior during the transients and to enable a more applicable zeroth-order adaptation, it is fundamental to scale the functions properly. When we do not know the cost functions a priori, it is difficult to scale the constraints. To address this potential numerical issue, we propose a gain adaptation scheme based on hybrid dynamical systems. In simple words, we design an outer-semicontinuous mapping which turns on the increase of the gain k_j when there is some level of constraint violation $g_j(\boldsymbol{u}) \geq 2\epsilon$, and turns it off when the constraint violation is minimal $g_j(\boldsymbol{u}) \leq \epsilon$, or when the gain reaches the maximum value $\bar{k}$. The collective flow set and flow map for $\xi := \mathrm{col}(\boldsymbol{u}, \boldsymbol{z}, \lambda, w, k, s)$ read as:

$$\xi \in C := \mathbb{R}^{2m} \times \mathbb{R}_+^{2q} \times \mathcal{K}^q \times \mathcal{S}^q \tag{13a}$$

$$\begin{bmatrix} \dot{\boldsymbol{u}} \\ \dot{\boldsymbol{z}} \\ \dot{\lambda} \\ \dot{w} \\ \dot{k} \\ \dot{s} \end{bmatrix} = F(\xi) := \begin{bmatrix} -\boldsymbol{u} + \boldsymbol{z} - \Gamma(F(\boldsymbol{u}) + \nabla g(\boldsymbol{u})^\top \lambda) \\ -\boldsymbol{z} + \boldsymbol{u} \\ \mathrm{diag}(k)\,\mathrm{diag}(\lambda)\,(g(\boldsymbol{u}) - \lambda + w) \\ -w + \lambda \\ \frac{1}{2} c\, S^2(\mathbf{1} + s) \\ \mathbf{0} \end{bmatrix}, \tag{13b}$$

and the collective jump set and jump map

$$\xi \in D := \bigcup_{j=1}^{q} D_j, \quad D_j := \left(D_j^+ \cup D_j^- \cup D_j^0\right) \tag{14a}$$

$$\xi^+ \in G(\xi) := \left\{ \left(\bigcup^{j \in \mathcal{C}} G_j(\xi),\ \xi \in \bigcap^{j \in \mathcal{C}} D_j \right)_{\mathcal{C} \in \mathcal{P}(\mathcal{Q})} \right., \tag{14b}$$

where k is a vector of gains for the dual dynamics; $\mathcal{K} := [\underline{k}, \bar{k}]$ is the set of possible values for these gains; s is a vector of discrete states which indicate if the gains in k are increasing or not; $\mathcal{S} := \{-1, 0, 1\}$ is the set of possible discrete states; $c > 0$ is positive constant which regulates the increase of k; $S := \mathrm{diag}(s)$, $\epsilon > 0$ is a positive number, $D_j^+ := \{\boldsymbol{u} \mid g_j(\boldsymbol{u}) \geq 2\epsilon\} \times \mathbb{R}^m \times \mathbb{R}_+^{2q} \times \mathcal{K}^q \times \mathcal{S}^{j-1} \times \{-1\} \times \mathcal{S}^{q-j}$ is the set which triggers the increasing k_j dynamics; $D_j^- := \{\boldsymbol{u} \mid g_j(\boldsymbol{u}) \leq \epsilon\} \times \mathbb{R}^m \times \mathbb{R}_+^{2q} \times \mathcal{K}^q \times \mathcal{S}^{j-1} \times \{1\} \times \mathcal{S}^{q-j}$ is the set which triggers the stopping of the k_j dynamics; $D_j^0 := \mathbb{R}^{2m} \times \mathbb{R}_+^{2q} \times \mathcal{K}^{j-1} \times \{\bar{k}\} \times \mathcal{K}^{q-j} \times \mathcal{S}^{j-1} \times \{-1, 1\} \times \mathcal{S}^{q-j}$ is the set which triggers the permanent stop of k_j dynamics; $\mathcal{P}(\mathcal{X})$ is the set of all subsets of $\mathcal{X}$; the jump maps $G_j(\xi)$ are defined as

$$G_j(\xi) := \begin{cases} \Delta_{-j}\xi - \Delta_j \xi, & \xi \in D_j^+ \cup D_j^- \\ \Delta_{-j}\xi, & \xi \in D_j^0 \\ \{\Delta_{-j}\xi - \Delta_j, \Delta_{-j}\xi\}, & \xi \in (D_j^+ \cup D_j^-) \cap D_j^0 \end{cases}$$

where Δ_j is a diagonal matrix with all zeros on the diagonal, except for the row corresponding to the s_j state which is equal to one and $\Delta_{-j} := I - \Delta_j$.

The set-valued definitions are necessary for outer-semicontinuity, which in turn via hybrid systems theory provides us with some robustness properties. An example trajectory can be seen in Fig. 2. We note that due to the design of the jump sets, no jumps can occur in a sufficiently small neighborhood of a GNE, and no solution can have an infinite number of jumps, as formalized next:

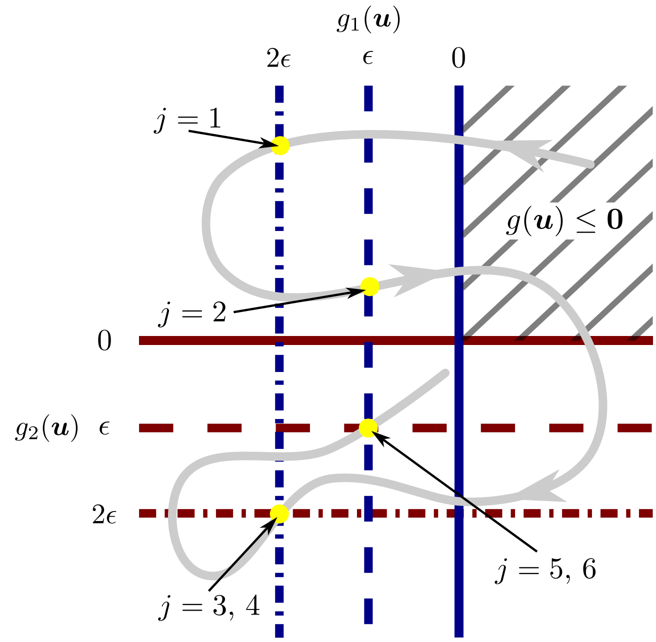

Fig. 2. The trajectory is denoted with a gray line, events with yellow dots, first constraint with red and second with blue lines. The trajectory starts in the set where constraints are satisfied ($g(\boldsymbol{u}) \leq 0$). The first event is triggered when the trajectory leaves the set where $g_1(\boldsymbol{u}) < 2\epsilon$, causing the state s_1 to change to 1 which then starts the increase of k_1 gain. The second event happens when the trajectory returns to the set where $g_1(\boldsymbol{u}) \leq \epsilon$ and the state s_1 is reset to 0 which halts the increase in gains. Events 3 and 4 happen when the trajectory leaves the sets $g_1(\boldsymbol{u}) < 2\epsilon$ and $g_2(\boldsymbol{u}) < 2\epsilon$ simultaneously. In that case, in random order, states s_1 and s_2 are set to 1. The last jumps happen when the trajectory simultaneously enters the sets $g_1(\boldsymbol{u}) \leq \epsilon$ and $g_2(\boldsymbol{u}) \leq \epsilon$. Again, the states s_1 and s_2 are reset to 0 in random order. (For interpretation of the references to color in this figure legend, the reader is referred to the web version of this article.)

Lemma 2. *Let the Standing Assumptions hold and let $\xi(t, j)$ be a complete solution to the hybrid system (C, D, F, G) in (13a), (13b), (14a) and (14b). Then, $\xi(t, j)$ has a finite number of jumps.* □

Proof. See Appendix C. ■

Apart from the gain adaptation scheme, the main difference between the dynamics in (13) and those in (10) is the fact that the flow mapping of the dual variables contains the new gain vector. Thus, one would expect similar behavior compared to that in (10). Furthermore, thanks to the hybrid basic assumptions, our system in (13) does not become unstable for arbitrarily small noise, as formalized in the following definition and robust convergence result for our hybrid adaptive algorithm.

Definition 4 (*Structural Robustness Poveda & Li, 2021*)**.** Let a compact set $\mathcal{A}$ be UGpAS (resp. SGPpAS as $\varepsilon \to 0^+$) for the hybrid system $\mathcal{H}$ with $\beta \in \mathcal{KL}$. We say that $\mathcal{H}$ is Structurally Robust if for all measurable functions $e : \mathbb{R}_{\geq 0} \to \mathbb{R}^n$ satisfying $\sup_{t \geq 0} \|e(t)\| \leq \bar{e}$, with $\bar{e} > 0$, the perturbed system

$$x + e \in C, \qquad \dot{x} = F(x + e) + e \tag{15a}$$

$$x + e \in D, \qquad x^+ = G(x + e) + e \tag{15b}$$

renders the set $\mathcal{A}$ SGPpAS as $\bar{e} \to 0^+$ (resp. SGPpAS as $(\varepsilon, \bar{e}) \to 0^+$) with $\beta \in \mathcal{KL}$. □

Theorem 2. *Let the Standing Assumptions hold and consider the hybrid system (C, D, F, G) in (13a), (13b), (14a) and (14b). Then, for any initial condition such that $\xi(0,0) \notin \mathcal{L} \times \mathcal{K}^q \times \mathcal{S}^q$ there exists a compact set $\mathscr{K} \supset \mathcal{A} \times \mathcal{K}^q \times \mathcal{S}^q$, such that the set $\mathcal{A} \times \mathcal{K}^q \times \mathcal{S}^q$ is UGAS for the restricted hybrid system $(C \cap \mathscr{K}, D \cap \mathscr{K}, F, G)$. Additionally, the restricted system is structurally robust.* □

Proof. See Appendix D. ■

4. Zeroth-order generalized Nash equilibrium seeking

The main assumptions of Algorithms in Sections 3.1 and 3.2 are that each agent knows their partial-gradient mapping and the actions of other agents. Such knowledge can be difficult to acquire in practical applications (Ariyur & Krstic, 2003). Our proposed zeroth-order GNE seeking algorithm requires a much weaker assumption; we assume that each agent is only able to measure their cost function. To estimate the pseudogradient via the measurements, we introduce additional oscillator states $\boldsymbol{\mu}$. By injecting oscillations into the inputs of the cost functions, it is possible to estimate the pseudogradient. For example of a real function of a single variable, it holds that $f(x + a\sin(t))\sin(t) \approx f(x)\sin(t) + a\nabla f(x)\sin^2(t)$ for small a. If the right-hand expression is averaged in time, only $\frac{a}{2}\nabla f(x)$ remains as the desired estimate. The principle is the same for mappings. In order to reduce oscillations, the estimate is then passed through a first-order filter with state $\boldsymbol{\zeta}$ and forwarded into the algorithm in Section 3.2 instead of the real pseudogradient.

Our new algorithm for the collective state $\phi := \mathrm{col}(\boldsymbol{u}, \boldsymbol{z}, \lambda, w, k, s, \boldsymbol{\zeta}, \boldsymbol{\mu})$ is given by

$$\phi \in C_0 := C \times \mathbb{R}^m \times \mathbb{S}^m \tag{16a}$$

$$\begin{bmatrix} \dot{\boldsymbol{u}} \\ \dot{\boldsymbol{z}} \\ \dot{\lambda} \\ \dot{w} \\ \dot{k} \\ \dot{s} \\ \dot{\boldsymbol{\zeta}} \\ \dot{\boldsymbol{\mu}} \end{bmatrix} = F_0(\phi) := \begin{bmatrix} \boldsymbol{\nu}\boldsymbol{\varepsilon}\left(-\boldsymbol{u} + \boldsymbol{z} - \Gamma(\boldsymbol{\zeta} + \nabla g(\boldsymbol{u})^\top \lambda)\right) \\ \boldsymbol{\nu}\boldsymbol{\varepsilon}\left(-\boldsymbol{z} + \boldsymbol{u}\right) \\ \nu_0\varepsilon_0 \,\mathrm{diag}(k)\,\mathrm{diag}(\lambda)\,(g(\boldsymbol{u}) - \lambda + w) \\ \nu_0\varepsilon_0\left(-w + \lambda\right) \\ \frac{1}{2}\nu_0\varepsilon_0 c\, S^2(\mathbf{1} + s) \\ \mathbf{0} \\ \boldsymbol{\nu}\left(-\boldsymbol{\zeta} + \hat{F}(\boldsymbol{u}, \boldsymbol{\mu})\right) \\ 2\pi\mathcal{R}_\kappa \boldsymbol{\mu} \end{bmatrix} \tag{16b}$$

where $\zeta_i \in \mathbb{R}^{m_i}$, $\mu_i \in \mathbb{S}^{m_i}$ are the oscillator states, $\varepsilon_i, \nu_i \geq 0$ for all $i \in \mathcal{I}_0 := \mathcal{I} \cup \{0\}$, $\boldsymbol{\varepsilon} := \mathrm{blkdiag}\left((\varepsilon_i I_{m_i})_{i\in\mathcal{I}}\right)$, $\boldsymbol{\gamma} := \mathrm{blkdiag}\left((\gamma_i I_{m_i})_{i\in\mathcal{I}}\right)$, $\mathcal{R}_\kappa := \mathrm{blkdiag}\left((\mathcal{R}_i)_{i\in\mathcal{I}}\right)$, $\mathcal{R}_i := \mathrm{blkdiag}\left(\left(\left[\begin{smallmatrix} 0 & -\kappa_j \\ \kappa_j & 0 \end{smallmatrix}\right]\right)_{j\in\mathcal{M}_i}\right)$, $\kappa_i > 0$ for all i and $\kappa_i \neq \kappa_j$ for $i \neq j$, $\mathcal{M}_i := \{\sum_{j=1}^{i-1} m_j + 1, \dots, \sum_{j=1}^{i-1} m_j + m_i\}$ is the set of indices corresponding to the state u_i, $\mathbb{D}^n \in \mathbb{R}^{n\times 2n}$ is a matrix that selects every odd row from the vector of size $2n$, $a_i > 0$ are small perturbation amplitude parameters, $A := \mathrm{blkdiag}\left((a_i I_{m_i})_{j\in\mathcal{I}}\right)$, $J(\boldsymbol{u}) = \mathrm{blkdiag}\left((J_i(u_i, \boldsymbol{u}_{-i}) I_{m_i})_{i\in\mathcal{I}}\right)$, and $\hat{F}(\boldsymbol{u}, \boldsymbol{\mu}) = 2A^{-1}J(\boldsymbol{u} + A\mathbb{D}^m\boldsymbol{\mu})\mathbb{D}^m\boldsymbol{\mu}$. The flow set and map are defined as

$$D_0 := D \times \mathbb{R}^m \times \mathbb{S}^m \tag{17a}$$

$$\phi^+ \in G_0(\phi) := \begin{bmatrix} G(\xi) \\ \xi \\ \mu \end{bmatrix}. \tag{17b}$$

The existence of solutions follows directly from (Goebel, Sanfelice, & Teel, 2009, Prop. 6.10) as the continuity of the right-hand side in (16), (17) and the definitions of flow and jump sets imply (Goebel et al., 2009, Assum. 6.5). As for most extremum seeking schemes with constant perturbation, convergence to a neighborhood of the solutions can be guaranteed. Thus, let us introduce the corresponding stability concept, the so called semi-global practical asymptotic stability.

Definition 5 (*SG(p)AS Poveda et al., 2018*)**.** For a parameterized HDS $\mathcal{H}_\varepsilon$, $\varepsilon \in \mathbb{R}^k_+$, a compact set $\mathcal{A} \subset \mathbb{R}^n$ is said to be Semi-Globally Practically pre-Asymptotically Stable (SGPpAS) as $(\varepsilon_1, \dots, \varepsilon_k) \to 0^+$ with $\beta \in \mathcal{KL}$ if for all compact sets $K \subset \mathbb{R}^n$ and all $\upsilon > 0$, there exists $\varepsilon_0^* > 0$ such that for each $\varepsilon_0 \in \left(0, \varepsilon_0^*\right)$ there exists $\varepsilon_1^*(\varepsilon_0) > 0$ such that for each $\varepsilon_1 \in \left(0, \varepsilon_1^*(\varepsilon_0)\right) \dots$ there exists $\varepsilon_j^*\left(\varepsilon_{j-1}\right) > 0$ such that for each $\varepsilon_j \in \left(0, \varepsilon_j^*\left(\varepsilon_{j-1}\right)\right) \dots, j = \{2, \dots, k\}$, every solution x_ε of $\mathcal{H}_\varepsilon$ with $x_\varepsilon(0,0) \in K$ satisfies

$$\|x_\varepsilon(t,j)\|_{\mathcal{A}} \leq \beta\left(\|x_\varepsilon(0,0)\|_{\mathcal{A}}, t+j\right) + \upsilon$$

for all $(t,j) \in \mathrm{dom}\,(x_\varepsilon)$. If additionally all solutions are complete, we then have Semi-Globally Practically Asymptotically Stable (SGPAS). □

Our main technical result of this section is summarized in the following theorem.

Theorem 3. *Let the Standing Assumptions hold and consider the hybrid system (C_0, D_0, F_0, G_0) in (16) and (17). Then, for any initial condition such that $\phi(0,0) \notin \mathcal{L} \times \mathcal{K}^q \times \mathcal{S}^q \times \mathbb{R}^m \times \mathbb{S}^m$ there exists a compact set $\mathscr{K} \supset \mathcal{A} \times \mathcal{K}^q \times \mathcal{S}^q \times \mathbb{R}^m \times \mathbb{S}^q$, such that the set $\mathcal{A} \times \mathcal{K}^q \times \mathcal{S}^q \times \mathbb{R}^m \times \mathbb{S}^q$ is SGPAS as $(\bar{a}, \bar{\varepsilon}, \bar{\nu}) = (\max_{i\in\mathcal{I}} a_i, \max_{i\in\mathcal{I}_0} \varepsilon_i, \max_{i\in\mathcal{I}_0} \nu_i) \to 0$ for the restricted hybrid system $((C \cap \mathscr{K}) \times \mathbb{R}^m \times \mathbb{S}^m), ((D \cap \mathscr{K}) \times \mathbb{R}^m \times \mathbb{S}^m, F_0, G_0)$. Additionally, the restricted system is structurally robust.* □

Proof. See Appendix E. ■

Remark 2. For the sake of brevity, we made some assumptions on the structure of our proposed algorithms. Namely, we assume that the amplitudes of the perturbation signals a_i are constant, that the frequencies of the perturbation signals are different for every state, and that every state of the pseudogradient is estimated. Analogous results hold for slowly-varying amplitudes $a_i(t) \in [\underline{a}, \bar{a}]$ where the upper and lower bounds are design parameters, for perturbation signals with the same frequency but sufficiently different phases so that "learning" can occur, and for the pseudogradient with some, but not all, estimated coordinates. □

5. Numerical simulations

5.1. Two-player monotone game

For illustration purposes, let us consider a two-player monotone game with the following cost functions

$$J_1(\boldsymbol{u}) = (u_1 - 2)(u_2 - 3)$$

$$J_2(\boldsymbol{u}) = -(u_1 - 2)(u_2 - 3), \tag{18}$$

and constraints

$$u_1 \geq u_2 + 1 \text{ and } u_1 \geq 4. \tag{19}$$

Game in (18) and (19) has a unique GNE $(u_1^*, u_2^*) = (4, 3)$ and is known to be divergent for algorithms that require strong monotonicity of the pseudogradient. As simulation parameters we choose $c = 10$, $k_j(0,0) = 1$, $\lambda_j = 0.1$ for all $i \in \mathcal{I}$, $j \in \mathcal{Q}$, $k_{\min} = 1$, $k_{\max} = 10^5$, $(u_1(0,0), u_2(0,0)) = (10, 0)$, and all other initial parameters were set to zero. We compare the algorithm in (13), (14) with algorithm in (10) for different values of the gain and show the numerical simulations in Figs. 3, 4, 5. In Figs. 3 and 4, it seems that the trajectory with the highest gain does not converge to the equilibrium. However, this is not the case since

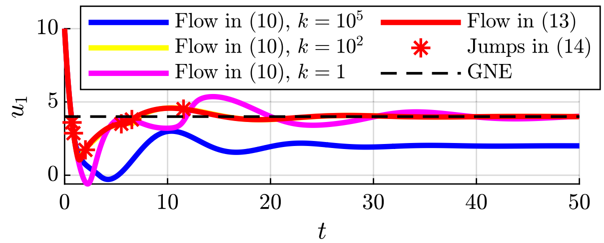

(a) Time evolution of states u_1 for the cases with and without ($k_{\min} = k_{\max}$) adaptive gain in (13).

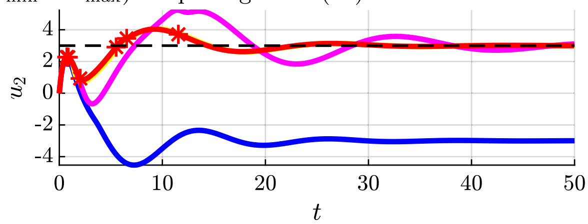

(b) Time evolution of states u_2 for the cases with and without ($k_{\min} = k_{\max}$) adaptive gain in (13).

Fig. 3. The trajectory with the adaptive gain is almost identical to the trajectory with gain $k = 100$. (For interpretation of the references to color in this figure legend, the reader is referred to the web version of this article.)

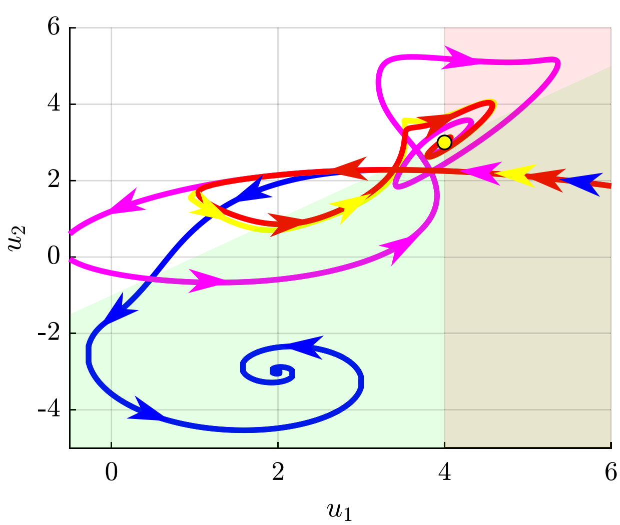

Fig. 4. Trajectories with (red) and without (blue, magenta, yellow) adaptive gain in a phase plane. The yellow dot represents the GNE, while the other colored lines are denoted as in Fig. 3. (For interpretation of the references to color in this figure legend, the reader is referred to the web version of this article.)

the Lagrangian multipliers converge very close to zero during the initial part of the trajectory when both the constraints are satisfied. Thus, as the multipliers themselves act as a "gain" in the dynamics, it takes longer for the dynamics to evolve towards the desired equilibrium. Eventually, the Lagrangian multipliers will grow large enough to let the trajectory start moving towards a solution. Furthermore, we note that the trajectory for the gain $k = 1$ is the second slowest with respect to convergence speed. Thus, in this scenario, choosing the gain either too small or too large is detrimental to the convergence speed. On the other hand, our adaptive gain behaves similarly as the case of gain $k = 100$, which is the "optimally tuned" gain. In Figs. 4 and 5, we denote the area where the constraints are satisfied with green and red rectangles. In Fig. 6, we see how the adaptive gain turns on and off based on the constraint violation.

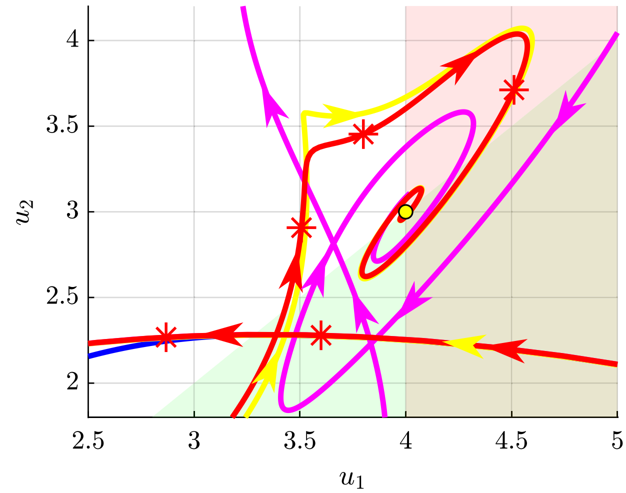

Fig. 5. Trajectories in the neighborhood of the GNE (yellow dot). The jumps are activated when entering and leaving the half-spaces corresponding to the constraints (red and transparent green). The color code is as in Fig. 3: blue for constant gain $k = 10^5$, yellow for constant gain $k = 10^2$, purple for constant gain $k = 1$, and red for adaptive gain. (For interpretation of the references to color in this figure legend, the reader is referred to the web version of this article.)

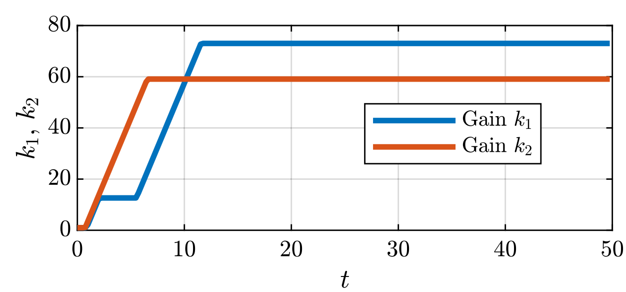

Fig. 6. Time evolution of the gains k_1 and k_2.

5.2. Perturbation signal optimization in oil extraction

Oil extraction becomes financially unviable when the reservoir pressure drops under a certain threshold. To solve this problem, one can employ gas-lifting (Silva & Pavlov, 2020). Compressed gas is injected down the well to decrease the density of the fluid and the hydrostatic pressure, causing an increase in production. The oil rate is typically a concave hard-to-model function of the gas injection rate (Silva & Pavlov, 2020) with a maximum that slowly changes over time due to changing conditions, making it an excellent candidate for extremum seeking. Extraction sites usually have multiple wells that are operated by the same processing facility. The goal is to maximize the oil extraction rate

$$J_1(\boldsymbol{x}) = \sum_{i=1}^{N} f_i(x_i), \tag{20}$$

while not exceeding a linear coupling constraint which may relate to total injection rate, power load, etc.

$$\sum_{i}^{N} b_i x_i \leq x_{\max}, \tag{21}$$

where $f_i : \mathbb{R} \to \mathbb{R}$ and $x_i \in \mathbb{R}$ are the oil-rate function and the injection rate, respectively, of the well i and $b_i, x_{\max} \in \mathbb{R}$. We denote the solution to this problem as x^*. Furthermore, the processing facility wants to reduce the oscillations in the total optimal extraction rate that result from the extremum seeking perturbation signals:

$$\hat{x}_i(t) = x_i(t) + d_i(t) = x_i(t) + a_i \sin(\omega t + \phi_i). \tag{22}$$

The oscillations of a single well's optimal extraction rate can be approximated as

$$f_i(\hat{x}_i) - f_i(x_i) \approx \nabla f_i(x_i)\, a_i \sin(\omega t + \phi_i).$$

The secondary goal cannot be accomplished by techniques that diminish the oscillation amplitude over time (Abdelgalil & Taha, 2021; Bhattacharjee & Subbarao, 2021) as the cost functions are slowly-varying and the learning procedure would stop prematurely. Furthermore, we cannot use too high frequencies (Suttner, 2019) as that would also destroy our equipment. Thus, to accomplish our goal, wells are grouped into pairs (i, j), and each pair selects perturbation signals which are in antiphase:

$$\begin{aligned} d_i(t) &= a_i \sin(\omega t + \phi_i) \\ d_j(t) &= -a_j \sin(\omega t + \phi_i). \end{aligned} \tag{23}$$

Without the coupling constraint and with an even number of wells, the perturbation signals in (23) reduce the oscillations in the neighborhood of the optimum as $\nabla f_1(x_1^*) \approx \nabla f_2(x_2^*) \approx \cdots \approx \nabla f_N(x_N^*) \approx 0$. However, if a constraint is present, the perturbation signals might not cancel out properly, because for some pair (i, j) it can hold that $\nabla f_i(x_i^*) \not\approx \nabla f_j(x_j^*)$. Therefore, it is also necessary to adapt the amplitudes a_i, a_j to improve the cancellation effect. Without loss of generality, we assume that neighboring indices are paired up as in (23). The secondary cost function is formulated as follows:

$$\hat{J}_2(a) = \frac{l}{2}\sum_{i=1}^{\frac{N}{2}} \left(\nabla f_{2i}(x_{2i}^*)\, a_{2i} - \nabla f_{2i-1}(x_{2i-1}^*)\, a_{2i-1}\right)^2 - \sum_{i=1}^{N} \log_p\left((a_i - \underline{a})(\overline{a} - a_i)\right)$$

where $l > 0$, $\underline{a}$ and $\overline{a}$ are the minimum and maximum perturbation amplitude respectively, and it holds $0 < \underline{a} < \overline{a}$. We denote $a^* := \operatorname{argmin} \hat{J}_2(a)$. Since x^* is not known in advance, direct computation of a^* is not possible. One can modify the previous cost function to use any value of x

$$J_2(x, a) = \frac{l}{2}\sum_{i=1}^{\frac{N}{2}} \left(\nabla f_{2i}(x_{2i})\, a_{2i} - \nabla f_{2i-1}(x_{2i-1})\, a_{2i-1}\right)^2, - \sum_{i=1}^{N} \log_p\left((a_i - \underline{a})(\overline{a} - a_i)\right), \tag{24}$$

and minimize the cost function:

$$J_p(x, a) = -\alpha J_1(x) + \beta J_2(x, a), \quad \alpha, \beta > 0, \tag{25}$$

with constraint (21). However, this approach only approximates the solution (x^*, a^*) for $\alpha \gg \beta$. With our game-theoretic formulation instead, we look for a solution (x^*, a^*) such that x^* is an optimal solution to the oil extraction problem in (20) and the overall pair (x^*, a^*) is variational GNE, meaning that the amplitudes are fairly and optimally chosen. To show that the game is monotone and can be solved by our algorithm, it is sufficient to show that the Jacobian matrix of the pseudogradient is positive semidefinite (Rockafellar & Wets, 2009, Prop. 12.3):

$$\mathcal{J}_F(x, a) := \begin{bmatrix} \mathcal{J}_{11} & \mathcal{J}_{12} \\ \mathcal{J}_{21} & \mathcal{J}_{22} \end{bmatrix} \succcurlyeq 0. \tag{26}$$

The submatrix $\mathcal{J}_{11} := \operatorname{blkdiag}\left((-\nabla^2 f_i(x_i))_{i\in\mathcal{I}}\right)$ is positive semidefinite as all of the cost functions in (20) are concave. Furthermore, the submatrix $\mathcal{J}_{12}$ is a zero matrix as the concave cost functions do not depend on the perturbation amplitudes. Then it holds that $\mathcal{J}_{22} := \operatorname{blkdiag}\left(\mathcal{J}_{1,2}, \mathcal{J}_{3,4}, \ldots, \mathcal{J}_{N-1,N}\right)$, where

$$\mathcal{J}_{i,j} = l\begin{bmatrix} (\nabla f_i(x_i))^2 & -\nabla f_i(x_i)\nabla f_j(x_j) \\ -\nabla f_i(x_i)\nabla f_j(x_j) & \left(\nabla f_j(x_j)\right)^2 \end{bmatrix} + \begin{bmatrix} \frac{(a_i-\overline{a})^{-2} + (a_i-\underline{a})^{-2}}{\log(p)} & 0 \\ 0 & \frac{(a_j-\overline{a})^{-2} + (a_j-\underline{a})^{-2}}{\log(p)} \end{bmatrix}. \tag{27}$$

As both matrices in (27) are positive semidefinite, and $\mathcal{J}_{22}$ is block diagonal, it follows that the matrix $\mathcal{J}_{22}$ is positive semidefinite. Finally, due to the block triangular structure of $\mathcal{J}_F$ and positive semidefinitness of $\mathcal{J}_{11}$ and $\mathcal{J}_{22}$, we conclude that $\mathcal{J}_F$ is positive semidefinite and in turn that the pseudogradient is monotone.

In our example, the amplitudes of the perturbation signals are part of the decision variable and are therefore time-varying; all perturbation signals have the same frequency but different phases (23); and coordinates of the pseudogradient related to cost functions in (24) need not be estimated, but can be computed directly. Thus, by Remark 2, we suitably adjust the algorithm in (16), (17) and use it for our numerical simulations. Furthermore, we use the well oil extraction rates as in (Silva & Pavlov, 2020)

$$\begin{aligned} f_1(x_1) = &- 3.9 \times 10^{-7} x_1^4 + 2.1 \times 10^{-4} x_1^3 \\ &- 0.043 x_1^2 + 3.7 x_1 + 12, \\ f_2(x_2) = &- 1.3 \times 10 - 7 x_2^4 + 10^{-4} x_2^3 \\ &- 2.8 \times 10^{-2} x_2^2 + 3.1 x_2 - 17, \\ f_3(x_3) = &- 1.2 \times 10^{-7} x_3^4 + 10^{-4} x_3^3 \\ &- 0.028 x_3^2 + 2.5 x_3 - 16, \\ f_4(x_4) = &- 4 \times 10^{-7} x_4^4 + 1.8 \times 10^{-4} x_4^3 \\ &- 0.036 x_4^2 + 3.5 x_4 + 10, \end{aligned}$$

and the following parameters: $l = 10$, $\nu_i = 0.1$, $\varepsilon_i = 0.01$ for all i, $\overline{a} = 10$, $\underline{a} = 5$, $p = 100$, $\epsilon = 10$, $\omega_i = 1$, $x_{\max} = 200$, $b_1 = 1$, $b_2 = 2$, $b_3 = 3$, $b_4 = 4$, $k_{\min} = 0.01$, $k_{\max} = 10\,000$, $c = 1000$, $\Gamma = 10$. For initial conditions: $\boldsymbol{u}(0) = \boldsymbol{z}(0) = \operatorname{col}(10, 10, 10, 10, 7.5, 7.5, 7.5, 7.5)$, $w(0) = 0$, $\lambda(0) = 0.1$, $\zeta(0) = \mathbf{0}$, $k(0) = 0.01$, $s(0) = 0$. Additionally, we run numerical simulations where only the total oil rate is optimized with constant perturbation amplitudes $a_i = 5$, using again the algorithm in (16). In Fig. 7, we see that the amplitude optimization indeed reduces the amplitude of the oscillations in the oil rate by 51% in the steady state, even though larger amplitudes were used in the perturbation signals. In Fig. 8, we can see how the constraints are violated over time. After half an hour, the constraints are always marginally satisfied. In Fig. 9, we note that in each pair, one of the amplitudes converges to a neighborhood of the minimal value.

6. Conclusion

Monotone generalized Nash equilibrium problems with dualized constraints can be solved via the continuous-time golden ratio algorithm augmented by projection-less dual dynamics. Furthermore, the algorithm can be adapted via hybrid systems theory for use with zeroth-order information feedback.

Appendix A. Proof of Theorem 1

We choose the following Lyapunov function candidate

$$V(\omega, \omega^*) = \frac{1}{2}\left\|\boldsymbol{u} - \boldsymbol{u}^*\right\|_{\Gamma^{-1}}^2 + \frac{1}{2}\left\|\boldsymbol{z} - \boldsymbol{z}^*\right\|_{\Gamma^{-1}}^2 + \frac{1}{2}\left\|w - w^*\right\|^2 + \sum_{j\in\mathcal{Q}}\left(\lambda_j - \lambda_j^* - \lambda_j^* \log\left(\frac{\lambda_j{}^*}{\lambda_j}\right)\right), \tag{A.1}$$

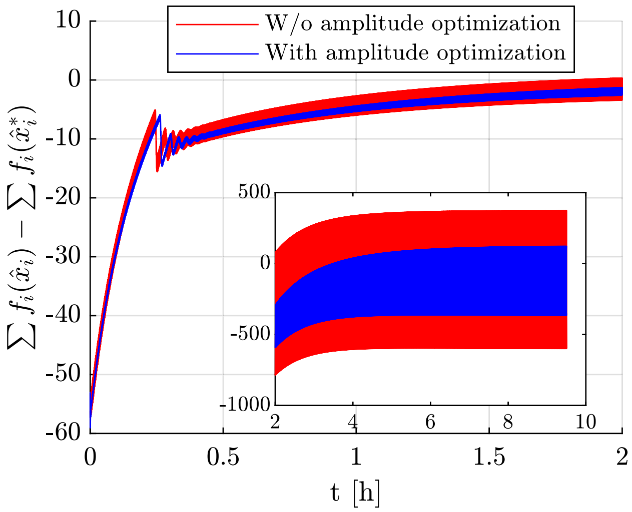

Fig. 7. Time evolution of the total oil extraction rate for the case with and without perturbation amplitude optimization. Amplitude optimization results in a 51% steady state oscillation reduction.

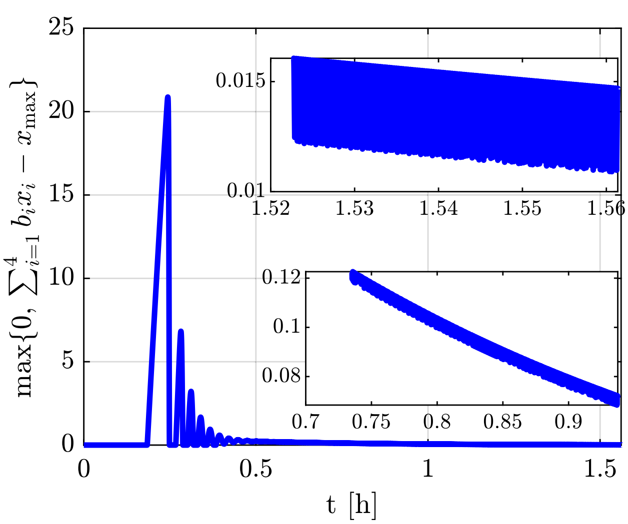

Fig. 8. Constraint violation over time.

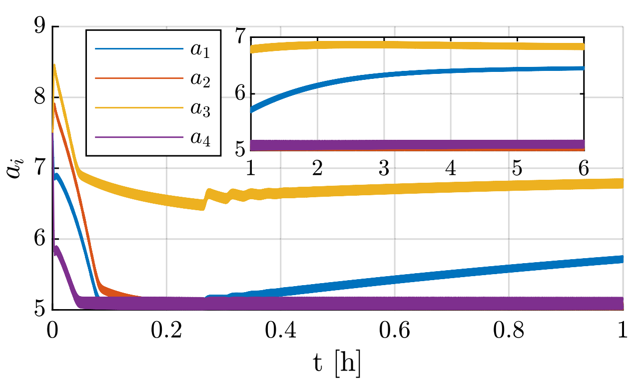

Fig. 9. Time evolution of amplitudes a_i.

where $\omega^* \in \mathcal{A}$ is any equilibrium point of (10) whose $\boldsymbol{u}^*, \lambda^*$ states correspond to a GNE and we define $0 \log 0 := 0$. The first three terms represent a weighted Euclidean distance from the solution $(\boldsymbol{u}^*, \boldsymbol{z}^*, w^*)$. As in Dürr and Ebenbauer (2011) and Dürr, Zeng et al. (2013), the fourth addend is chosen such that its Lyapunov derivative is the same as in the case of the standard norm $\|\lambda - \lambda^*\|$ and standard dynamics $\dot{\lambda} = -\lambda + \mathrm{proj}_{\mathbb{R}_+}(g(\boldsymbol{u}) - \lambda)$. By Standard Assumption 4, equilibrium points in $\mathcal{M} \setminus \mathcal{A}$ are disconnected from $\mathcal{A}$. Furthermore, going back to the Lyapunov function, points in $\mathcal{M} \setminus \mathcal{A}$ are not in its domain, and by proving negative semi-definiteness of the Lyapunov derivative, their potential region of attraction is reduced to set $\mathcal{L} \supset \mathcal{M}$. Thus, we do not consider points in $\mathcal{L}$ for initial conditions. The Lyapunov derivative is given by

$$
\begin{aligned}
\dot{V} &= \left\langle \boldsymbol{u} - \boldsymbol{u}^* \mid \Gamma^{-1}\left(-\boldsymbol{u} + \boldsymbol{z} - \Gamma(F(\boldsymbol{u}) + \nabla g(\boldsymbol{u})^\top \lambda)\right)\right\rangle \\
&\quad + \left\langle \boldsymbol{z} - \boldsymbol{u}^* \mid \Gamma^{-1}(-\boldsymbol{z} + \boldsymbol{u})\right\rangle + \left\langle w - \lambda^* \mid -w + \lambda \right\rangle \\
&\quad + \sum_{j \in \mathcal{Q}} \left(\dot{\lambda}_j - \tfrac{\lambda_j^*}{\lambda_j}\dot{\lambda}_j\right) \\
&\le -\|\boldsymbol{u} - \boldsymbol{z}\|^2_{\Gamma^{-1}} - \left\langle \boldsymbol{u} - \boldsymbol{u}^* \mid F(\boldsymbol{u}) + \nabla g(\boldsymbol{u})^\top \lambda \right\rangle \\
&\quad \left\langle w - \lambda^* \mid -w + \lambda \right\rangle + \sum_{j \in \mathcal{Q}} (\lambda_j - \lambda_j)^* (g_j(\boldsymbol{u}) - \lambda_j + \omega_j) \\
&\le -\|\boldsymbol{u} - \boldsymbol{z}\|^2_{\Gamma^{-1}} - \left\langle \boldsymbol{u} - \boldsymbol{u}^* \mid F(\boldsymbol{u}) + \nabla g(\boldsymbol{u})^\top \lambda \right\rangle \\
&\quad + \left\langle w - \lambda^* \mid -w + \lambda \right\rangle + \left\langle \lambda - \lambda^* \mid g(\boldsymbol{u}) - \lambda + w \right\rangle \\
&\le -\|\boldsymbol{u} - \boldsymbol{z}\|^2_{\Gamma^{-1}} - \|\lambda - w\|^2 + \left\langle \lambda - \lambda^* \mid g(\boldsymbol{u}) \right\rangle \\
&\quad + \left\langle \boldsymbol{u} - \boldsymbol{u}^* \mid F(\boldsymbol{u}) + \nabla g(\boldsymbol{u})^\top \lambda \right\rangle .
\end{aligned} \tag{A.2}
$$

From the properties of v-GNE set, we conclude that

$$
\begin{aligned}
&\boldsymbol{0}_m = F\left(\boldsymbol{u}^*\right) + \nabla g(\boldsymbol{u}^*)^\top \lambda^* \\
&0 = \left\langle \boldsymbol{u} - \boldsymbol{u}^* \mid F\left(\boldsymbol{u}^*\right) + \nabla g(\boldsymbol{u}^*)^\top \lambda^* \right\rangle \\
&0 \le \left\langle g(\boldsymbol{u}^*) \mid \lambda^* - \xi \right\rangle \text{ for all } \xi \in \mathbb{R}^q_+
\end{aligned} \tag{A.3}
$$

Thus, by using (A.3) within (A.2), we further derive

$$
\begin{aligned}
\dot{V} &\le -\|\boldsymbol{u} - \boldsymbol{z}\|^2_{\Gamma^{-1}} - \|\lambda - w\|^2 - \left\langle \boldsymbol{u} - \boldsymbol{u}^* \mid F(\boldsymbol{u}) - F(\boldsymbol{u}^*)\right\rangle \\
&\quad - \left\langle \boldsymbol{u} - \boldsymbol{u}^* \mid \nabla g(\boldsymbol{u})^\top \lambda - \nabla g(\boldsymbol{u}^*)^\top \lambda^* \right\rangle \\
&\quad + \left\langle \lambda - \lambda^* \mid g(\boldsymbol{u}) - g(\boldsymbol{u}^*)\right\rangle \\
&\le -\|\boldsymbol{u} - \boldsymbol{z}\|^2_{\Gamma^{-1}} - \|\lambda - w\|^2 - \underbrace{\left\langle \boldsymbol{u} - \boldsymbol{u}^* \mid F(\boldsymbol{u}) - F(\boldsymbol{u}^*)\right\rangle}_{\le 0} \\
&\quad + \sum_{j \in \mathcal{Q}} \underbrace{\lambda_j}_{\ge 0} \underbrace{\left(g_j(\boldsymbol{u}) - g_j(\boldsymbol{u}^*) + \left\langle \boldsymbol{u}^* - \boldsymbol{u} \mid \nabla g_j(\boldsymbol{u})\right\rangle\right)}_{\le 0} \\
&\quad - \sum_{j \in \mathcal{Q}} \underbrace{\overset{*}{\lambda_j}}_{\ge 0} \underbrace{\left(g_j(\boldsymbol{u}) - g_j(\boldsymbol{u}^*) - \left\langle \boldsymbol{u} - \boldsymbol{u}^* \mid \nabla g_j(\boldsymbol{u}^*)\right\rangle\right)}_{\ge 0} \\
&\le -\|\boldsymbol{u} - \boldsymbol{z}\|^2_{\Gamma^{-1}} - \|\lambda - w\|^2 ,
\end{aligned} \tag{A.4}
$$

where the last inequality follows from the monotonicity of the pseudogradient and the convexity of the coupled constraints. Now, we prove via La Salle's theorem that the trajectories of (10) converge to the set $\mathcal{A}$. Let us define the following sets:

$$
\begin{aligned}
\Omega_c &:= \{\omega \in \mathbb{R}^{2m} \times \mathbb{R}^{2q}_+ \mid V(\omega) \le c\} \\
\Omega_0 &:= \{\omega \in \Omega_c \mid \boldsymbol{u} = \boldsymbol{z} \text{ and } \lambda = w\} \\
\mathcal{Z} &:= \{\omega \in \Omega_c \mid \dot{V}(\omega) = 0\} \\
\mathcal{O} &:= \{\omega \in \Omega_c \mid \omega(0) \in \mathcal{Z} \Rightarrow \omega(t) \in \mathcal{Z}\ \forall t \in \mathbb{R}\},
\end{aligned} \tag{A.5}
$$

where Ω_c is a non-empty compact sublevel set of the Lyapunov function candidate, $\mathcal{Z}$ is the set of zeros of its derivative, Ω_0 is the superset of $\mathcal{Z}$ which follows from (A.4) and $\mathcal{O}$ is the maximum invariant set as explained in Khalil (2002, Chp. 4.2). Then, for some $c > 0$ large enough, it holds that

$$
\Omega_c \supseteq \Omega_0 \supseteq \mathcal{Z} \supseteq \mathcal{O} \supseteq \mathcal{A}. \tag{A.6}
$$

Firstly, for any compact set Ω_c, since the right-hand side of (10) is (locally) Lipschitz continuous and therefore by Khalil (2002, Thm. 3.3) we conclude that solutions to (10) exist and are unique. Next, we show that the only ω-limit trajectories in $\mathcal{O}$ are the equilibrium points of the dynamics in (10), i.e. $\mathcal{O} \equiv \mathcal{A}$. It is sufficient to prove that there cannot exist any positively invariant trajectories in Ω_0, apart from stationary points in $\mathcal{A}$. For trajectories in Ω_0, it holds that

$$\mathbf{0} = \boldsymbol{u} - \boldsymbol{z} \tag{A.7}$$

$$\mathbf{0} = \dot{\boldsymbol{u}} - \dot{\boldsymbol{z}} \tag{A.8}$$

$$\mathbf{0} = \lambda - w \tag{A.9}$$

$$\mathbf{0} = \dot{\lambda} - \dot{w}, \tag{A.10}$$

and therefore

$$\mathbf{0} = F(\boldsymbol{u}) + \nabla g(\boldsymbol{u})^\top \lambda \tag{A.11}$$

$$\mathbf{0} = \operatorname{diag}(\lambda)\, g(\boldsymbol{u}), \tag{A.12}$$

where (A.11) follows from (10) and (A.8), and (A.12) follows from (10), (A.9) and (A.10). Eqs. (A.8), (A.9), (A.11) and (A.12) form the definition of set $\mathcal{M}$ in (11) and the fact that $\mathcal{M} \setminus \mathcal{A}$ is not in the domain, we conclude $\Omega_0 \equiv \mathcal{A}$. Since the set $\mathcal{O}$ is a subset of the set Ω_0, we conclude that $\mathcal{O} \equiv \mathcal{A}$. Therefore, by La Salle's theorem (Khalil, 2002, Thm. 4), set $\mathcal{A}$ is attractive for the dynamics in (10).

Next, we prove the stability of $\mathcal{A}$. We restrict the domain of the dynamics by choosing an arbitrary ω^* and a set Λ that contains arbitrarily many initial conditions of interest not contained in the set $\mathcal{L}$, and it holds $\mathcal{A} \subset \Lambda$. Then, we compute $\overline{c} = \max_{\omega \in \Lambda} V(\omega, \omega^*)$ and define the new restricted domain to the forward invariant set $\mathscr{E}$, where $\mathscr{E} := \{\omega \in \mathbb{R}^{2m} \times \mathbb{R}^{2q}_+ \mid V(\omega, \omega^*) \leq \overline{c}\}$.

Consequently, we define the following set-valued mapping of compact sets

$$\Omega(\omega^*, c) := \{\omega \in \mathscr{E} \mid V(\omega, \omega^*) \leq c\}.$$

Now, we prove global stability with respect to the set $\mathcal{A}$ by showing that any Lyapunov invariant set can be upper and lower bounded by balls surrounding the solution set. Let us choose an arbitrary $\varepsilon > 0$. For a particular c and ω^*, since V does not increase, it follows that all trajectories that start in $\Omega(\omega^*, c)$ are contained in the set. Let us choose $c(\omega^*)$ such that $\Omega(\omega^*, c(\omega^*)) \subseteq (\mathcal{A} + \varepsilon\mathbb{B}) \cap \mathscr{E}$. By continuity of V, for every set $\Omega(\omega^*, c(\omega^*))$, it is possible to find $\delta(\omega^*) > 0$ such that $(\omega^* + \delta(\omega^*)\mathbb{B}) \cap \mathscr{E} \subseteq \Omega(\omega^*, c(\omega^*))$. If we take $\delta = \min_{\omega^* \in \mathcal{A}} \delta(\omega^*)$, it holds that $\cup_{\omega^* \in \mathcal{A}} (\omega^* + \delta\mathbb{B}) \cap \mathscr{E} = (\mathcal{A} + \delta\mathbb{B}) \cap \mathscr{E}$. Thus, $(\mathcal{A} + \delta\mathbb{B}) \cap \mathscr{E} \subseteq \cup_{\omega^* \in \mathcal{A}} \Omega(\omega^*, c(\omega^*))$ which implies that all solutions with $\omega(0) \in (\mathcal{A} + \delta\mathbb{B})$, remain in $(\mathcal{A} + \varepsilon\mathbb{B})$ for all $t \geq 0$. Therefore, set $\mathcal{A}$ is globally stable and attractive on $\mathscr{E}$, hence it is UGAS.

Appendix B. Proof of Lemma 1

We study the stability of singular equilibrium points in the set $\mathcal{M} \setminus \mathcal{A}$. The main difference between the set $\mathcal{M} \setminus \mathcal{A}$ and the set of solutions $\mathcal{A}$, is that the set $\mathcal{M} \setminus \mathcal{A}$ contains points where $\overline{\lambda}_j = 0$ and $g_i(\overline{\boldsymbol{u}}) > 0$ for some index j. Let $\hat{\omega} \in \mathcal{M} \setminus \mathcal{A}$. Without loss of generality, we assume that for $j = q$ it holds that $\hat{\lambda}_q = 0$ and $g_q(\hat{\boldsymbol{u}}) > 0$. In order to check the stability of the point $\hat{\omega}$, we study the dynamics in (10) linearized around $\hat{\omega}$:

$$\begin{bmatrix} \dot{\tilde{\boldsymbol{z}}} \\ \dot{\tilde{\boldsymbol{u}}} \\ \dot{\tilde{w}} \\ \dot{\tilde{\lambda}} \end{bmatrix} = \left[\begin{array}{ccc|c} -I_m & I_m & \mathbf{0} & \mathbf{0} \\ I_m & -I_m - M & \mathbf{0} & -\nabla g(\hat{\boldsymbol{u}})^\top \\ \mathbf{0} & \mathbf{0} & -I_q & I_q \\ 0 & 0 & 0 & g_1(\hat{\boldsymbol{u}}) \\ \vdots & \vdots & \vdots & \vdots \\ \hline 0 & 0 & 0 & g_q(\hat{\boldsymbol{u}}) \end{array}\right] \begin{bmatrix} \tilde{\boldsymbol{z}} \\ \tilde{\boldsymbol{u}} \\ \tilde{w} \\ \tilde{\lambda} \end{bmatrix}, \tag{B.1}$$

where $\tilde{\boldsymbol{z}} := \boldsymbol{z} - \hat{\boldsymbol{z}}$, $\tilde{\boldsymbol{u}} := \boldsymbol{u} - \hat{\boldsymbol{u}}$, $\tilde{w} := w - \hat{w}$, $\tilde{\lambda} := \lambda - \hat{\lambda}$ and $M(\hat{\boldsymbol{u}}, \hat{\lambda}) := \frac{\partial}{\partial \boldsymbol{u}} \left(\Gamma(F(\boldsymbol{u}) + \nabla g(\boldsymbol{u})^\top \lambda)\right)\big|_{\boldsymbol{u}=\hat{\boldsymbol{u}}, \lambda=\hat{\lambda}}$. The system matrix will have at least one positive eigenvalue due to the upper triangular structure and the element $g_q(\hat{\boldsymbol{u}}) > 0$ in the last row. It follows that the equilibrium point $\hat{\omega}$ is unstable for dynamics in (10). As $\hat{\omega}$ was chosen arbitrarily, we conclude that any equilibrium point in $\mathcal{M} \setminus \mathcal{A}$ is unstable.

Appendix C. Proof of Lemma 2

Let us assume otherwise, that we have an infinite amount of jumps. By the structure of the jump set and map, we must jump between $s_i = -1$ and $s_i = 1$ an infinite amount of times for at least one of the states i. Without the loss of generality, we assume that this is true for $i = j$. As we can spend only a finite amount of time in the state $s_j = 1$ ($\tau = \frac{\overline{k} - \underline{k}}{c_j}$), time between jumps from $s_j = 1$ to $s_j = -1$, t_k, has to decrease to zero, otherwise $\sum^{\infty} t_k = \infty > \tau$. Minimum time between jumps $t_{\min}$ is equal to $\frac{d_{\min}}{\max \|\dot{\boldsymbol{u}}\|}$, where $d_{\min}$ is the minimal distance between the jump sets corresponding to $s_j = -1$ and $s_j = 1$, and $\max \|\dot{\boldsymbol{u}}\|$ is finite based on the continuity of the flow map and the forward invariance of any compact set Ω_c.

To show that $d_{\min} \neq 0$, let $G_j(\epsilon) := \{\boldsymbol{y} \mid g_j(\boldsymbol{y}) = \epsilon\}$ and choose ϵ such that $G_j(2\epsilon) \neq \emptyset$. By convexity property of the constraint function, for $\boldsymbol{u} \in G_j(\epsilon)$ and $\boldsymbol{v} \in G_j(2\epsilon)$, we have:

$$\begin{aligned} g_j(\boldsymbol{u}) &\geq g_j(\boldsymbol{v}) + \nabla g_j(\boldsymbol{v})(\boldsymbol{u} - \boldsymbol{v}) \\ \epsilon &\leq \nabla g_j(\boldsymbol{v})(\boldsymbol{v} - \boldsymbol{u}) \leq \left\|\nabla g_j(\boldsymbol{v})\right\| \|\boldsymbol{v} - \boldsymbol{u}\|. \\ \frac{\epsilon}{\left\|\nabla g_j(\boldsymbol{v})\right\|} &\leq \|\boldsymbol{v} - \boldsymbol{u}\| \end{aligned}$$

As the set $G_j(2\epsilon)$ is compact, and $\nabla g_j(\boldsymbol{v})$ is continuous in its coordinates, by the extreme value theorem, $\left\|\nabla g_j(\boldsymbol{v})\right\|$ reaches a maximum δ on that set. Therefore, the minimum distance is bounded below as $d_{\min} \geq \frac{\epsilon}{\delta}$. As both $d_{\min}$ and $\|\dot{\boldsymbol{u}}\|$ are finite positive numbers, we conclude that $t_{\min} > 0$, which leads us to a contradiction. Therefore, we can only have a finite number of jumps. ■

Appendix D. Proof of Theorem 2

Proof of convergence is similar to that of Theorem 1. First, we note that the additional states are invariant to the set $\mathcal{K}^q \times \mathcal{S}^q$ regardless of the rest of the dynamics. Next, we choose the Lyapunov function candidate

$$\begin{aligned} V(\omega, \omega^*, k) &= \tfrac{1}{2}\left\|\boldsymbol{u} - \boldsymbol{u}^*\right\|^2_{\Gamma^{-1}} + \tfrac{1}{2}\left\|\boldsymbol{z} - \boldsymbol{u}^*\right\|^2_{\Gamma^{-1}} \\ &+ \tfrac{1}{2}\left\|w - \lambda^*\right\|^2 + \sum_{j \in \mathcal{Q}} \tfrac{1}{k_j}\left(\lambda_j - \lambda_j^* - \lambda_j^* \log\left(\tfrac{\lambda_j^*}{\lambda_j}\right)\right), \end{aligned} \tag{D.1}$$

which depends on the chosen equilibrium point ω^*. In a similar manner as in the proof of Theorem 1, it follows that

$$u_c(\xi) = \langle \nabla V(\xi) \mid F(\xi) \rangle \leq -\|\boldsymbol{u} - \boldsymbol{z}\|^2_{\Gamma^{-1}} - \|\lambda - w\|^2, \tag{D.2}$$

$$u_d(\xi) = V(\omega_+, \omega^*, k) - V(\omega, \omega^*, k) = 0. \tag{D.3}$$

We restrict the flow and jump sets by choosing an arbitrary ω^* and set Λ that contains arbitrarily many initial conditions of interest not contained in the set $\mathcal{L}$, and it holds $\mathcal{A} \subset \Lambda$. Then, we compute $\overline{c} = \max_{\omega \in \Lambda} V(\omega, \omega^*, k_{\max})$ and define the new restricted flow set as $\mathscr{K} := \mathscr{E} \times \mathcal{K}^q \times \mathcal{S}^q$, where $\mathscr{E} := \{\omega \in \mathbb{R}^{2m} \times \mathbb{R}^{2q}_+ \mid V(\omega, \omega^*, k_{\min}) \leq \overline{c}\}$.

Consequently, we define the following set-valued mapping of compact sets

$$\Omega(\omega^*, k, c) := \{\omega \in \mathscr{E} \mid V(\omega, \omega^*, k) \leq c\}.$$

In comparison to the invariant sets of Theorem 1, the compacts sets also depend on the adaptive gains. In fact, it holds that $\mathbf{0} < k' \leq k''$ implies that $\Omega(\omega^*, k', c) \subseteq \Omega(\omega^*, k'', c)$. As k is dynamic, the "invariant set", in which the trajectories of ω dynamics are contained, expands in the λ dimensions. Due to the fact that the minimal and maximal values of the gain are algorithm parameters, the "expansion" of the set is bounded.

Now, we show global stability with respect to the set $\mathcal{A} \times \mathcal{K}^q \times \mathcal{S}^q$ by showing that any invariant set can be upper and lower bounded by a ball surrounding the solution set, when accounting for the "inflation" of the set due to changes of the gain. Let us choose an arbitrary $\varepsilon > 0$. For a particular c and ω^*, the trajectories are constrained to the largest Ω set for $k = k_{\max}$, and to the smallest for $k = k_{\min}$. Therefore, by the fact that V does not increase during flows or jumps, and that the gains k are constrained to the set $\mathcal{K}^q$, it follows that all trajectories that start in $\Omega(\omega^*, k_{\min}, c)$ are contained in the set $\Omega(\omega^*, k_{\max}, c)$.

Let us choose $c(\omega^*)$ such that $\Omega(\omega^*, k_{\max}, c(\omega^*)) \subseteq (\mathcal{A} + \varepsilon\mathbb{B}) \cap \mathscr{E}$. By continuity of V, for every set $\Omega(\omega^*, k_{\min}, c(\omega^*))$, it is possible to find $\delta(\omega^*) > 0$ such that $(\omega^* + \delta(\omega^*)\mathbb{B}) \cap \mathscr{E} \subseteq \Omega(\omega^*, k_{\min}, c(\omega^*))$. If we take $\delta = \min_{\omega^* \in \mathcal{A}} \delta(\omega^*)$, it holds that $\cup_{\omega^* \in \mathcal{A}} (\omega^* + \delta\mathbb{B}) \cap \mathscr{E} = (\mathcal{A} + \delta\mathbb{B}) \cap \mathscr{E}$. Thus, $(\mathcal{A} + \delta\mathbb{B}) \cap \mathscr{E} \subseteq \cup_{\omega^* \in \mathcal{A}} \Omega(\omega^*, k_{\min}, c(\omega^*))$ which implies that all maximal solutions with $\xi(0,0) \in (\mathcal{A}+\delta\mathbb{B}) \times \mathcal{K}^q \times \mathcal{S}^q$, remain in $(\mathcal{A}+\varepsilon\mathbb{B}) \times \mathcal{K}^q \times \mathcal{S}^q$ for all $(t,j) \in \mathrm{dom}\xi$.

Next, we prove global attractivity for the constrained flow and jump sets. Let ξ be a complete solution in $\mathscr{K}$. For a fixed ω^*, we define $\hat{V}(\xi) := V(\omega, \omega^*, k)$. Via (Goebel et al., 2012, Cor. 8.7) and Lemma 2, we conclude that for some $r \geq 0$, ξ approaches the largest weakly invariant subset in $\hat{V}^{-1}(r) \cap \mathscr{K} \cap \overline{u_c^{-1}(0)}$, where the notation $f^{-1}(r)$ stands for the r-level set of f on $\mathrm{dom} f$, the domain of definition of f, i.e., $f^{-1}(r) := \{z \in \mathrm{dom} f \mid f(z) = r\}$. By same reasoning as in Theorem 1, we conclude that $\overline{u_c^{-1}(0)} = \mathcal{A} \times \mathcal{K}^q \times \mathcal{S}^q$.

Thus, the largest weakly invariant subset for ξ reads as $\hat{V}^{-1}(r) \cap (\mathcal{A} \times \mathcal{K}^q \times \mathcal{S}^q)$. Every trajectory ξ converges to a different subset. The union of invariant subsets for every trajectory is $\mathcal{A} \times \mathcal{K}^q \times \mathcal{S}^q$, as we can choose an initial condition for which it holds $\omega(0,0) = \omega^* = const.$ for all $(t,j) \in \mathrm{dom}\xi$, for any $\omega^* \in \mathcal{A}$.

Therefore, $\mathcal{A} \times \mathcal{K}^q \times \mathcal{S}^q$ is globally attractive, as all solutions are complete, which implies that the set $\mathcal{A} \times \mathcal{K}^q \times \mathcal{S}^q$ is UGAS (Goebel et al., 2012, Thm. 7.12) on the restricted flow and jump sets. Furthermore, by Poveda and Li (2021, Prop. A.1.), the HDS $(C \cap \mathscr{K}, D \cap \mathscr{K}, F, G)$ is structurally robust.

Appendix E. Proof of Theorem 3

We rewrite the system in (16b) as

$$\begin{bmatrix} \dot{\boldsymbol{u}} \\ \dot{\boldsymbol{z}} \\ \dot{\lambda} \\ \dot{w} \\ \dot{k} \\ \dot{s} \\ \dot{\boldsymbol{\zeta}} \end{bmatrix} = \begin{bmatrix} \bar{\nu}\bar{\varepsilon}\tilde{\boldsymbol{\nu}}\tilde{\boldsymbol{\varepsilon}} \left(-\boldsymbol{u} + \boldsymbol{z} - \Gamma(\boldsymbol{\zeta} + \nabla g(\boldsymbol{u})^\top \lambda)\right) \\ \bar{\nu}\bar{\varepsilon}\tilde{\boldsymbol{\nu}}\tilde{\boldsymbol{\varepsilon}} \left(-\boldsymbol{z} + \boldsymbol{u}\right) \\ \bar{\nu}\bar{\varepsilon}\tilde{\nu}_0\tilde{\varepsilon}_0 \operatorname{diag}(k) \operatorname{diag}(\lambda) \left(g(\boldsymbol{u}) - \lambda + w\right) \\ \bar{\nu}\bar{\varepsilon}\tilde{\nu}_0\tilde{\varepsilon}_0 \left(-w + \lambda\right) \\ \frac{1}{2}\bar{\nu}\bar{\varepsilon}\tilde{\nu}_0\tilde{\varepsilon}_0 c(I+S)S^2 \\ \mathbf{0} \\ \bar{\nu}\tilde{\boldsymbol{\nu}} \left(-\boldsymbol{\zeta} + \hat{F}(\boldsymbol{u}, \boldsymbol{\mu})\right) \end{bmatrix}, \tag{E.1}$$

$$\dot{\boldsymbol{\mu}} = 2\pi \mathcal{R}_\kappa \boldsymbol{\mu}, \tag{E.2}$$

where $\bar{\nu} := \max_{i \in \mathcal{I}_0} \nu_i$, $\bar{\varepsilon} := \max_{i \in \mathcal{I}_0} \varepsilon_i$, $\tilde{\boldsymbol{\nu}} := \boldsymbol{\nu}/\bar{\nu}$, $\tilde{\boldsymbol{\varepsilon}} := \boldsymbol{\varepsilon}/\bar{\varepsilon}$, $\tilde{\nu}_0 := \nu_0/\bar{\nu}$ and $\tilde{\varepsilon}_0 := \varepsilon_0/\bar{\varepsilon}$. The system in (E.1), (E.2) is in singular perturbation from where $\bar{\nu}$ is the time scale separation constant. The goal is to average the dynamics of $\xi, \boldsymbol{\zeta}$ along the solutions of $\boldsymbol{\mu}$. For sufficiently small $\bar{a} := \max_{i \in \mathcal{I}} a_i$, we can use the Taylor expansion to write down the cost functions as

$$J_i(\boldsymbol{u} + A\mathbb{D}\boldsymbol{\mu}) = J_i(u_i, \boldsymbol{u}_{-i}) + a_i(\mathbb{D}^{m_i}\mu_i)^\top \nabla_{u_i} J_i(u_i, \boldsymbol{u}_{-i}) + A_{-i}(\mathbb{D}^{m-i}\boldsymbol{\mu}_{-i})^\top \nabla_{u_{-i}} J(u_i, \boldsymbol{u}_{-i}) + O(\bar{a}^2), \tag{E.3}$$

where $A_{-i} := \operatorname{blkdiag}\left((a_i I_{m_i})_{j \in \mathcal{I}\setminus\{i\}}\right)$. By the fact that the right-hand side of (E.1), (E.2) is continuous, by using (Poveda & Krstić, 2021, Lemma 2) and by substituting (E.3) into (E.1), we derive the well-defined average of the complete dynamics:

$$\begin{bmatrix} \dot{\boldsymbol{u}} \\ \dot{\boldsymbol{z}} \\ \dot{\lambda} \\ \dot{w} \\ \dot{k} \\ \dot{s} \\ \dot{\boldsymbol{\zeta}} \end{bmatrix} = \begin{bmatrix} \bar{\varepsilon}\tilde{\boldsymbol{\nu}}\tilde{\boldsymbol{\varepsilon}} \left(-\boldsymbol{u} + \boldsymbol{z} - \Gamma(\boldsymbol{\zeta} + \nabla g(\boldsymbol{u})^\top \lambda)\right) \\ \bar{\varepsilon}\tilde{\boldsymbol{\nu}}\tilde{\boldsymbol{\varepsilon}} \left(-\boldsymbol{z} + \boldsymbol{u}\right) \\ \bar{\varepsilon}\tilde{\nu}_0\tilde{\varepsilon}_0 \operatorname{diag}(\lambda) \left(g(\boldsymbol{u}) - \lambda + w\right) \\ \bar{\varepsilon}\tilde{\nu}_0\tilde{\varepsilon}_0 \left(-w + \lambda\right) \\ \frac{1}{2}\bar{\varepsilon}\tilde{\nu}_0\tilde{\varepsilon}_0 c(I+S)S^2 \\ \mathbf{0} \\ \tilde{\boldsymbol{\nu}} \left(-\boldsymbol{\zeta} + F(\boldsymbol{u}) + \mathcal{O}(\bar{a})\right) \end{bmatrix}. \tag{E.4}$$

The system in (E.4) is an $\mathcal{O}(\bar{a})$ perturbed version of:

$$\begin{bmatrix} \dot{\boldsymbol{z}} \\ \dot{\boldsymbol{u}} \\ \dot{w} \\ \dot{\lambda} \\ \dot{k} \\ \dot{s} \\ \dot{\boldsymbol{\zeta}} \end{bmatrix} = \begin{bmatrix} \bar{\varepsilon}\tilde{\boldsymbol{\nu}}\tilde{\boldsymbol{\varepsilon}} \left(-\boldsymbol{z} + \boldsymbol{u}\right) \\ \bar{\varepsilon}\tilde{\boldsymbol{\nu}}\tilde{\boldsymbol{\varepsilon}} \left(-\boldsymbol{u} + \boldsymbol{z} - \Gamma(\boldsymbol{\zeta} + \nabla g(\boldsymbol{u})^\top \lambda)\right) \\ \bar{\varepsilon}\tilde{\nu}_0\tilde{\varepsilon}_0 \left(-w + \lambda\right) \\ \bar{\varepsilon}\tilde{\nu}_0\tilde{\varepsilon}_0 \operatorname{diag}(\lambda) \left(g(\boldsymbol{u}) - \lambda + w\right) \\ \frac{1}{2}\bar{\varepsilon}\tilde{\nu}_0\tilde{\varepsilon}_0 c(I+S)S^2 \\ \mathbf{0} \\ \tilde{\boldsymbol{\nu}} \left(-\boldsymbol{\zeta} + F(\boldsymbol{u})\right) \end{bmatrix}. \tag{E.5}$$

For sufficiently small $\bar{\varepsilon}$, the system in (E.5) is in singular perturbation form with dynamics $\boldsymbol{\zeta}$ acting as fast dynamics. The boundary layer dynamics are given by

$$\dot{\boldsymbol{\zeta}}_{\mathrm{bl}} = \tilde{\boldsymbol{\nu}} \left(-\boldsymbol{\zeta}_{\mathrm{bl}} + F(\boldsymbol{u}_{\mathrm{bl}})\right) \tag{E.6}$$

For each fixed $\boldsymbol{u}_{\mathrm{bl}}$, $\{F(\boldsymbol{u}_{\mathrm{bl}})\}$ is an uniformly globally exponentially stable equilibrium point of the boundary layer dynamics. By Wang et al. (2012, Exm. 1), it holds that the system in (E.5) has a well-defined average system given by

$$\begin{bmatrix} \dot{\boldsymbol{z}} \\ \dot{\boldsymbol{u}} \\ \dot{w} \\ \dot{\lambda} \\ \dot{k} \\ \dot{s} \end{bmatrix} = \begin{bmatrix} \tilde{\boldsymbol{\nu}}\tilde{\boldsymbol{\varepsilon}} \left(-\boldsymbol{z} + \boldsymbol{u}\right) \\ \tilde{\boldsymbol{\nu}}\tilde{\boldsymbol{\varepsilon}} \left(-\boldsymbol{u} + \boldsymbol{z} - \Gamma(F(\boldsymbol{u}) + \nabla g(\boldsymbol{u})^\top \lambda)\right) \\ \tilde{\nu}_0\tilde{\varepsilon}_0 \left(-w + \lambda\right) \\ \tilde{\nu}_0\tilde{\varepsilon}_0 \operatorname{diag}(\lambda) \left(g(\boldsymbol{u}) - \lambda + w\right) \\ \frac{1}{2}\tilde{\nu}_0\tilde{\varepsilon}_0 c(I+S)S^2 \\ \mathbf{0} \end{bmatrix}. \tag{E.7}$$

To prove that the system in (E.7) renders the set $\mathcal{A} \times \mathcal{K}^q \times \mathcal{S}^q$ UGAS for restricted dynamics, we consider the following Lyapunov function candidate:

$$V(\xi, \omega^*) = \tfrac{1}{2} \left\|\boldsymbol{u} - \boldsymbol{u}^*\right\|^2_{(\tilde{\boldsymbol{\nu}}\tilde{\boldsymbol{\varepsilon}}\Gamma)^{-1}} + \tfrac{1}{2} \left\|\boldsymbol{z} - \boldsymbol{u}^*\right\|^2_{(\tilde{\boldsymbol{\nu}}\tilde{\boldsymbol{\varepsilon}}\Gamma)^{-1}} + \tfrac{1}{2\tilde{\nu}_0\tilde{\varepsilon}_0} \left\|w - \lambda^*\right\|^2 + \sum_{j \in \mathcal{Q}} \tfrac{1}{\tilde{\nu}_0\tilde{\varepsilon}_0 k_j} \left(\lambda_j - \lambda_j^* - \lambda_j^* \log\left(\tfrac{\lambda_j{}^*}{\lambda_j}\right)\right). \tag{E.8}$$

The convergence proof is equivalent to the proof of Theorem 2 and is omitted. We restrict the flow and jump sets as $C \cap \mathscr{K}$ and $D \cap \mathscr{K}$ respectively.

Next, by Wang et al. (2012, Thm. 2, Exm. 1), the dynamics in (E.5) render the set $\mathcal{A} \times \mathcal{K}^q \times \mathcal{S}^q \times \mathbb{R}^m$ SGPAS as ($\bar{\varepsilon} \to 0$). As the right-hand side of the equations in (E.5) is continuous, the system is a well-posed hybrid dynamical system (Goebel et al., 2009, Thm. 6.30) and therefore the $O(\bar{a})$ perturbed system in (E.4) renders the set $\mathcal{A} \times \mathcal{K}^q \times \mathcal{S}^q \times \mathbb{R}^m$ SGPAS as $(\bar{\varepsilon}, \bar{a}) \to 0$ (Poveda & Li, 2021, Prop. A.1). By noticing that the set $\mathbb{S}^m$ is UGAS under oscillator dynamics in (E.2) that generate a well-defined average system in (E.4), and by averaging results in Poveda and Krstić (2021, Lemma 2), we obtain that the dynamics in (16b) make the set $\mathcal{A} \times \mathcal{K}^q \times \mathcal{S}^q \times \mathbb{R}^m \times \mathbb{S}^m$ SGPAS as $(\bar{\varepsilon}, \bar{a}, \bar{\nu}) \to 0$ for the restricted flow and jump sets. Furthermore, by Poveda and Li (2021, Prop. A.1.), HDS $((C \cap \mathscr{K}) \times \mathbb{R}^m \times \mathbb{S}^m), ((D \cap \mathscr{K}) \times \mathbb{R}^m \times \mathbb{S}^m, F_0, G_0)$ is structurally robust.

References

Abdelgalil, Mahmoud, & Taha, Haithem (2021). Lie bracket approximation-based extremum seeking with vanishing input oscillations. *Automatica*, Article 109735.

Ariyur, Kartik B., & Krstic, Miroslav (2003). *Real-time optimization by extremum-seeking control*. John Wiley & Sons.

Bauschke, Heinz H., Combettes, Patrick L., et al. (2011). *Convex analysis and monotone operator theory in Hilbert spaces, Vol. 408* (2nd ed.). Springer.

Bhattacharjee, Diganta, & Subbarao, Kamesh (2021). Extremum seeking control with attenuated steady-state oscillations. *Automatica*, *125*, Article 109432.

Bianchi, Mattia, & Grammatico, Sergio (2021). Continuous-time fully distributed generalized Nash equilibrium seeking for multi-integrator agents. *Automatica*, *129*, Article 109660.

Bot, Radu Ioan, Csetnek, Ernö Robert, & Vuong, Phan Tu (2020). The forward-backward-forward method from continuous and discrete perspective for pseudo-monotone variational inequalities in Hilbert spaces. *European Journal of Operational Research*.

Censor, Yair, Gibali, Aviv, & Reich, Simeon (2011). The subgradient extragradient method for solving variational inequalities in Hilbert space. *Journal of Optimization Theory and Applications*, *148*(2), 318–335.

Dürr, Hans-Bernd, & Ebenbauer, Christian (2011). A smooth vector field for saddle point problems. In *2011 50th IEEE conference on decision and control and European control conference* (pp. 4654–4660).

Dürr, Hans-Bernd, Stanković, Miloš S., Ebenbauer, Christian, & Johansson, Karl Henrik (2013). Lie bracket approximation of extremum seeking systems. *Automatica*, *49*(6), 1538–1552.

Dürr, Hans-Bernd, Zeng, Chen, & Ebenbauer, Christian (2013). Saddle point seeking for convex optimization problems. *IFAC Proceedings Volumes*, *46*(23), 540–545.

Facchinei, Francisco, & Kanzow, Christian (2010). Generalized Nash equilibrium problems. *Annals of Operations Research*, *175*(1), 177–211.

Facchinei, Francisco, & Pang, Jong-Shi (2007). *Finite-dimensional variational inequalities and complementarity problems*. Springer Science & Business Media.

Frihauf, Paul, Krstic, Miroslav, & Basar, Tamer (2011). Nash equilibrium seeking in noncooperative games. *IEEE Transactions on Automatic Control*, *57*(5), 1192–1207.

Gadjov, Dian, & Pavel, Lacra (2019). Distributed GNE seeking over networks in aggregative games with coupled constraints via forward-backward operator splitting. In *IEEE 58th conference on decision and control* (pp. 5020–5025).

Gadjov, Dian, & Pavel, Lacra (2020). On the exact convergence to Nash equilibrium in monotone regimes under partial-information. In *2020 59th IEEE conference on decision and control* (pp. 2297–2302).

Ghaffari, Azad, Krstić, Miroslav, & Nešić, Dragan (2012). Multivariable Newton-based extremum seeking. *Automatica*, *48*(8), 1759–1767.

Goebel, Rafal, Sanfelice, Ricardo G., & Teel, Andrew R. (2009). Hybrid dynamical systems. *IEEE Control Systems Magazine*, *29*(2), 28–93.

Goebel, Rafal, Sanfelice, Ricardo G., & Teel, Andrew R. (2012). *Hybrid dynamical systems*. Princeton University Press.

Goto, Tatsuhiko, Hatanaka, Takeshi, & Fujita, Masayuki (2012). Payoff-based inhomogeneous partially irrational play for potential game theoretic cooperative control: Convergence analysis. In *IEEE American control conference* (pp. 2380–2387).

Grammatico, Sergio (2017). Dynamic control of agents playing aggregative games with coupling constraints. *IEEE Transactions on Automatic Control*, *62*(9), 4537–4548.

Grushkovskaya, Victoria, Zuyev, Alexander, & Ebenbauer, Christian (2018). On a class of generating vector fields for the extremum seeking problem: Lie bracket approximation and stability properties. *Automatica*, *94*, 151–160.

Khalil, Hassan K. (2002). *Nonlinear systems*. Prentice Hall,

Korpelevich, Galina M. (1976). The extragradient method for finding saddle points and other problems. *Matecon*, *12*, 747–756.

Krilašević, Suad, & Grammatico, Sergio (2021a). An extremum seeking algorithm for monotone Nash equilibrium problems. In *2021 IEEE conference on decision and control (CDC)*. IEEE.

Krilašević, Suad, & Grammatico, Sergio (2021b). Learning generalized Nash equilibria in multi-agent dynamical systems via extremum seeking control. *Automatica*, *133*, Article 109846.

Krstić, Miroslav, & Wang, Hsin-Hsiung (2000). Stability of extremum seeking feedback for general nonlinear dynamic systems. *Automatica*, *36*(4), 595–601.

Labar, Christophe, Garone, Emanuele, Kinnaert, Michel, & Ebenbauer, Christian (2019). Newton-based extremum seeking: A second-order Lie bracket approximation approach. *Automatica*, *105*, 356–367.

Li, Sen, Zhang, Wei, Lian, Jianming, & Kalsi, Karanjit (2015). Market-based coordination of thermostatically controlled loads—Part I: A mechanism design formulation. *IEEE Transactions on Power Systems*, *31*(2), 1170–1178.

Liao, Chwen-Kai, Manzie, Chris, Chapman, Airlie, & Alpcan, Tansu (2019). Constrained extremum seeking of a MIMO dynamic system. *Automatica*, *108*, Article 108496.

Lin, Wei, Qu, Zhihua, & Simaan, Marwan A. Distributed game strategy design with application to multi-agent formation control. In *53rd IEEE conference on decision and control* (pp. 433–438).

Liu, Shu-Jun, & Krstić, Miroslav (2011). Stochastic Nash equilibrium seeking for games with general nonlinear payoffs. *SIAM Journal on Control and Optimization*, *49*(4), 1659–1679.

Ma, Zhongjing, Callaway, Duncan S., & Hiskens, Ian A. (2011). Decentralized charging control of large populations of plug-in electric vehicles. *IEEE Transactions on Control Systems Technology*, *21*(1), 67–78.

Malitsky, Yura (2019). Golden ratio algorithms for variational inequalities. *Mathematical Programming*, 1–28.

Marden, Jason R., Arslan, Gürdal, & Shamma, Jeff S. (2009). Cooperative control and potential games. *IEEE Transactions on Systems, Man and Cybernetics, Part B (Cybernetics)*, *39*(6), 1393–1407.

Marden, Jason R., & Shamma, Jeff S. (2012). Revisiting log-linear learning: Asynchrony, completeness and payoff-based implementation. *Games and Economic Behavior*, *75*(2), 788–808.

Mohsenian-Rad, Amir-Hamed, Wong, Vincent WS, Jatskevich, Juri, Schober, Robert, & Leon-Garcia, Alberto (2010). Autonomous demand-side management based on game-theoretic energy consumption scheduling for the future smart grid. *IEEE Transactions on Smart Grid*, *1*(3), 320–331.

Poveda, Jorge I., & Krstić, Miroslav (2021). Nonsmooth extremum seeking control with user-prescribed fixed-time convergence. *IEEE Transactions on Automatic Control*, *66*(12), 6156–6163.

Poveda, Jorge I, Kutadinata, Ronny, Manzie, Chris, Nešić, Dragan, Teel, Andrew R, & Liao, Chwen-Kai (2018). Hybrid extremum seeking for black-box optimization in hybrid plants: An analytical framework. In *2018 IEEE conference on decision and control* (pp. 2235–2240). IEEE.

Poveda, Jorge I., & Li, Na (2021). Robust hybrid zero-order optimization algorithms with acceleration via averaging in time. *Automatica*, *123*, Article 109361.

Poveda, Jorge I., & Quijano, Nicanor (2015). Shahshahani gradient-like extremum seeking. *Automatica*, *58*, 51–59.

Poveda, Jorge I., & Teel, Andrew R. (2017a). A framework for a class of hybrid extremum seeking controllers with dynamic inclusions. *Automatica*, *76*, 113–126.

Poveda, Jorge I., & Teel, Andrew R. (2017b). A robust event-triggered approach for fast sampled-data extremization and learning. *IEEE Transactions on Automatic Control*, *62*(10), 4949–4964.

Rockafellar, R. Tyrrell, & Wets, Roger J.-B. (2009). *Variational analysis, Vol. 317*. Springer Science & Business Media.

Saad, Walid, Han, Zhu, Poor, H. Vincent, & Basar, Tamer (2012). Game-theoretic methods for the smart grid: Game-theoretic methods for the smart grid: An overview of microgrid systems, demand-side management, and smart grid communications. *IEEE Signal Processing Magazine*, *29*, 86–105.

Sanfelice, Ricardo G., & Teel, Andrew R. (2011). On singular perturbations due to fast actuators in hybrid control systems. *Automatica*, *47*(4), 692–701.

Shao, Guangru, Teel, Andrew R, Tan, Ying, Liu, Kun-Zhi, & Wang, Rui (2019). Extremum seeking control with input dead-zone. *IEEE Transactions on Automatic Control*, *65*(7), 3184–3190.

Silva, Thiago Lima, & Pavlov, Alexey (2020). Dither signal optimization for multi-agent extremum seeking control. In *2020 European control conference* (pp. 1230–1237). IEEE.

Suttner, Raik (2019). Extremum seeking control with an adaptive dither signal. *Automatica*, *101*, 214–222.

Wang, Wei, Teel, Andrew R., & Nešić, Dragan (2012). Analysis for a class of singularly perturbed hybrid systems via averaging. *Automatica*, *48*(6), 1057–1068.

Ye, Maojiao, Hu, Guoqiang, & Xu, Shengyuan (2020). An extremum seeking-based approach for Nash equilibrium seeking in N-cluster noncooperative games. *Automatica*, *114*, Article 108815.

Yi, Peng, & Pavel, Lacra (2019). An operator splitting approach for distributed generalized Nash equilibria computation. *Automatica*, *102*, 111–121.

Suad Krilašević is a Ph.D. candidate at the Delft Center for Systems and Control, TU Delft, The Netherlands. Born in Sarajevo, Bosnia and Herzegovina in 1995, he received his Bachelor's and Master's degree in Electronics and Automatic control engineering at the Faculty of Electrical Engineering, University of Sarajevo, in September of 2016 and 2018 respectively. His research interests include game theory, multi-agent systems, hybrid systems and extremum seeking.

Sergio Grammatico is an Associate Professor at the Delft Center for Systems and Control, TU Delft, The Netherlands. He received Bachelor, Master and Ph.D. degrees from the University of Pisa, Italy, in 2008, 2009, 2013, respectively. In 2012-2017, he held research positions at University of California Santa Barbara, USA, at ETH Zurich, Switzerland, and at TU Eindhoven, The Netherlands. Dr. Grammatico has been awarded the 2021 Roberto Tempo Best Paper Award. He is currently an Associate Editor of the IEEE Transactions on Automatic Control and IFAC Automatica. He was recipient of the Best Paper Award at the 2016 ISDG Int. Conf. on Network Games, Control and Optimization. He is currently an Associate Editor of the IEEE Trans. on Automatic Control (2018–present) and of Automatica (2020–present).